Eugene E. Lundquist

1296

NATIONAL ADVISORY COMMITTEE FOR AERONAUTICS

TECHNICAL NOTE

No. 1296

WIND-TUNNEL INVESTIGATION OF THE EFFECTS OF SURFACE-COVERING DISTORTION ON THE CHARACTERISTICS OF A FLAP HAVING UNDISTORTED CONTOUR MAINTAINED FOR VARIOUS DISTANCES AHEAD OF THE TRAILING EDGE

By Thomas A. Toll, M. J. Queijo, and Jack D. Brewer

Langley Memorial Aeronautical Laboratory
Langley Field, Va.

Washington

May 1947

NATIONAL ADVISORY COMMITTEE FOR AERONAUTICS

TECHNICAL NOTE NO. 1296

WIND-TUNNEL INVESTIGATION OF THE EFFECTS OF SURFACE-COVERING DISTORTION ON THE CHARACTERISTICS OF A FLAP HAVING UNDISTORTED CONTOUR MAINTAINED FOR VARIOUS DISTANCES AHEAD OF THE TRAILING EDGE

By Thomas A. Toll, M. J. Queijo, and Jack D. Brewer

SUMMARY

Tests were made of a modified NACA 65_1-012 airfoil having a 30-percent airfoil-chord flap with contours simulating various distorted surface-covering shapes for the purpose of investigating the practicability of reducing distortion effects to a negligible amount by maintaining the undistorted contour over a small part of the flap chord near the trailing edge. The effects of variations in Mach number from 0.20 to 0.40, of transition location, and of flap gap also were investigated.

The results of the investigation indicated that the effects of distortion on lift characteristics are small compared with the effects of distortion on hinge-moment characteristics and that approximately 75 percent of the effects of distortion on stick forces can be eliminated if distortion of the rear 20 percent of the flap chord is prevented by stiffening that part of the flap. When the flap had been thickened by distortion, opening a gap at the flap nose or placing transition strips near the airfoil leading edge generally caused the variations of hinge-moment coefficient with angle of attack and with flap deflection to become less negative. Variations in Mach number from 0.20 to 0.40 had only small effects on the hinge-moment characteristics of the undistorted flap or of the distorted flaps having the undistorted contour maintained over the rear 20 percent of the flap chord.

INTRODUCTION

Flight results published in a British paper of limited distribution and some wind-tunnel tests made in the Langley stability

tunnel have indicated that large changes in control-surface characteristics (particularly the hinge moments) may result from distortion of the control-surface contour while under aerodynamic load. The analysis presented in reference 1 shows that, in general, distortion amounts either to a change in camber of the control surface (camber distortion) or to a change in the thickness of the control surface (symmetrical distortion). Camber distortion affects the control-surface characteristics in a manner that is similar to the effect of deflecting a tab; whereas symmetrical distortion amounts essentially to a change in trailing-edge angle. Distortion of the camber type was shown in reference 1 to have much larger effects than distortion of the symmetrical type.

The type of distortion obtained on a specific control surface depends primarily on the location of vents or leakage holes. Camber distortion is most likely to occur when the internal pressure is approximately equal to the static pressure of the free air stream, and symmetrical distortion is most likely to occur when the internal pressure is highly positive or highly negative relative to the static pressure of the free air stream.

From aerodynamic considerations, the most satisfactory method of eliminating distortion effects is to provide the entire control surface with a rigid covering material. Such a control surface is likely to be quite heavy, however. The fact that control-surface hinge-moment characteristics are known to depend largely on the contour near the trailing edge has led to the suggestion made in a British paper of limited distribution that the greater part of the effects of distortion might be eliminated, with a moderate increase in weight, by providing a rigid covering material over only a small chordwise part of the control surface just forward of the trailing edge. Tests made by A. S. Halliday of Great Britain indicated that when distortion of the rear 25 percent of the control-surface chord is prevented, the variation of hinge-moment coefficient with angle of attack and with flap deflection is essentially independent of distortion of any other parts of the control surface.

The present tests, made in two-dimensional flow, were conducted for the purpose of investigating more thoroughly the practicability of reducing distortion effects to a negligible amount by maintaining the undistorted contour over a small part of the flap chord near the trailing edge. Tests were made of several types of distortion in addition to those made by Halliday and for each type characteristics were determined with 10 percent, 20 percent, and 30 percent of the flap chord held to the undistorted contour. The effects of variations in Mach number from 0.20 to 0.40, of transition location, and of flap gap also were investigated.

SYMBOLS

c_l	airfoil section lift coefficient
c_{h_f}	flap section hinge-moment coefficient
P_R	resultant balance-pressure coefficient $\left(P_{lower} - P_{upper}\right)$
P	pressure coefficient above or below flap seal
C_L	finite-span lift coefficient
C_h	finite-span hinge-moment coefficient
m_s	seal-moment ratio for internally balanced flap (ratio of balancing moment of flexible seal to balancing moment of thin-plate overhang)
δ^*	boundary-layer displacement thickness, feet
q	dynamic pressure of free stream, pounds per square foot
q_t	dynamic pressure at tail of airplane, pounds per square foot
c	airfoil section chord, feet
c_ϕ	fixed trailing-edge chord (chordwise distance from trailing edge over which undistorted contour is maintained), feet
c_f	flap section chord, feet
c_{bp}	balance-plate section chord (distance from flap hinge line to leading edge of the balance plate), feet
c_b	balance section chord (distance from flap hinge line to point midway between points of attachment of flexible seal of sealed internal balance), feet
c'	mean aerodynamic chord of wing, feet
$\overline{c}_e$	root-mean-square elevator chord, feet
b_e	elevator span, feet

t	airfoil section thickness at flap hinge line, feet
l	tail length (distance from center of gravity of airplane to aerodynamic center of horizontal tail), feet
S_w	wing area, square feet
S_t	horizontal-tail area, square feet
A_w	wing aspect ratio
A_t	horizontal-tail aspect ratio
x	chordwise distance from airfoil leading edge to any point on airfoil surface, feet
x'	chordwise distance from center of gravity of airplane to neutral point, feet
W	weight of airplane, pounds
α_o	airfoil section angle of attack, degrees
α	angle of attack of finite-span surface, degrees
δ_f	flap deflection, degrees
δ_e	elevator deflection, degrees
i_t	stabilizer angle, degrees
ϵ	downwash angle in vicinity of horizontal tail, degrees
R	Reynolds number
M	Mach number
K	ratio of control force in pounds to elevator hinge moment in foot pounds
ΔF_s	incremental stick force resulting from elevator distortion, pounds

$$c_{l_\alpha} = \left(\frac{\partial c_l}{\partial \alpha_o}\right)_{\delta_f}$$

$$c_{l_\delta} = \left(\frac{\partial c_l}{\partial \delta_f}\right)_{\alpha_o}$$

$$c_{h_\alpha} = \left(\frac{\partial c_h}{\partial \alpha_o}\right)_{\delta_f}$$

$$c_{h_\delta} = \left(\frac{\partial c_h}{\partial \delta_f}\right)_{\alpha_o}$$

$$P_{R_\alpha} = \left(\frac{\partial P_R}{\partial \alpha_o}\right)_{\delta_f}$$

$$P_{R_\delta} = \left(\frac{\partial P_R}{\partial \delta_f}\right)_{\alpha_o}$$

$$C_{L_\alpha} = \left(\frac{\partial C_L}{\partial \alpha}\right)_{\delta_e}$$

$$C_{L_\delta} = \left(\frac{\partial C_L}{\partial \delta_e}\right)_{\alpha}$$

$$c_{h_\alpha} = \left(\frac{\partial c_h}{\partial \alpha}\right)_{\delta_e}$$

$$c_{h_\delta} = \left(\frac{\partial c_h}{\partial \delta_e}\right)_{\alpha}$$

The subscripts outside the parenthesis of the foregoing partial derivatives indicate factors held constant during measurement of the derivatives.

Δc_{l_α}, Δc_l, . . . incremental values of parameters resulting from any given amount of distortion; for example,

$$\Delta c_{l_\alpha} = c_{l_{\alpha_{distorted}}} - c_{l_{\alpha_{undistorted}}}$$

$\Delta c_{l_\alpha}'$, $\Delta c_l'$, . . . incremental distortion parameters (the increments of slopes or of coefficients resulting from a distortion of one percent of the flap chord); for example,

$$\Delta c_{l_\alpha}' = \frac{c_{l_{\alpha_{distorted}}} - c_{l_{\alpha_{undistorted}}}}{\text{distortion in percent flap chord}}$$

where distortion is defined as the maximum deviation of a surface of a flap from the undistorted contour

APPARATUS AND TESTS

The tests of the present investigation were conducted in the $2\frac{1}{2}$-foot by 6-foot test section of the Langley stability tunnel. The model had a chord of 2 feet and spanned the throat of the tunnel. The part of the model forward of the 70-percent-chord station was constructed of laminated mahogany and had the ordinates of the NACA 65_1-012 airfoil section. The airfoil was equipped with a 30-percent-chord plain flap with a cylindrical steel nose and a steel central web. Flap contours, simulating various distorted surface-covering shapes, were obtained by attaching wood blocks to

the upper and lower surfaces of the steel web. (See fig. 1.) The assumed undistorted contour had flat sides extending from the trailing edge to the contour of the NACA 65_1-012 airfoil at the 70-percent-chord station. The trailing-edge angle was 14°. The ordinates of the modified airfoil are given in table I.

For convenience in presenting the results of this investigation, letter designations have been assigned to the various basic types of contour distortion. In the designations, F stands for flat, C for concave, and B for bulge. Each flap-contour designation consists of two letters; the first letter refers to the upper surface of the flap and the second letter refers to the lower surface of the flap. The various designations and the corresponding descriptions of the flap contours tested are presented in the following table:

Designation	Description of flap contours
FF	Both surfaces flat (no distortion)
CC	Both upper and lower surfaces concave
BB	Both upper and lower surfaces bulged
BC	Upper surface bulged and lower surface concave
BF	Upper surface bulged and lower surface flat
FC	Upper surface flat and lower surface concave

For each of the basic flap contours given in the foregoing table, the undistorted flap contour was maintained over parts of the flap chord extending 10 percent, 20 percent, and 30 percent of the flap chord from the trailing edge. The various contours investigated are illustrated in figure 1.

Both the concave and the bulged contours were constructed as shown in figure 2. In every case, the amount of distortion - that is, the maximum deviation of the distorted contour from the undistorted contour - was 2.33 percent of the flap chord. The distorted parts of the flap surfaces consisted of a straight section (parallel to the undistorted surface) joined to the undistorted surface by circular arcs. As the undistorted trailing-edge part was increased in length, the straight section of the distorted part was decreased in length; thus the maximum deviation of the distorted contour from the undistorted contour was maintained constant.

The part of the model forward of the flap hinge line was attached rigidly to end disks that were mounted flush with the tunnel walls. Clearance gaps of approximately 1/16 inch were left

between the ends of the flap and the disks. The tests included determinations of airfoil section lift coefficients, flap section hinge-moment coefficients, and resultant balance-pressure coefficients. The lift of the model was measured with an integrating manometer, hinge moments were measured with a calibrated spring balance, and the pressure difference (resultant balance pressure) across the flexible nose seal was measured with a single U-shaped manometer tube.

Most of the tests were made with transition strips attached to the model. The strips were prepared by cementing carborundum grains (No. 60) to the back of "Scotch" cellulose tape in a strip $\frac{1}{4}$-inch wide. The tape was attached to the upper and lower surfaces of the model so that the leading edges of the carborundum strips were at 2.0 percent of the chord.

The greater part of the tests were made at a Mach number of 0.34, although a few tests were made at Mach numbers of 0.20 and 0.40. The dynamic pressures and the test Reynolds numbers corresponding to these Mach numbers are given in the following table:

Mach number, M	Dynamic pressure, q (lbs/sq ft)	Reynolds number, R
0.20	59.4	2,845,000
.34	155.5	4,590,000
.40	211.5	5,380,000

In order to specify the conditions of the present tests somewhat more completely than can be done simply by giving values of the Mach number, the dynamic pressure, and the Reynolds number, a few measurements of the boundary layer on the upper surface of the model with the undistorted flap contour were made. Figure 3 shows the variation with angle of attack α_o of the boundary-layer displacement thickness at 65 percent of the chord, given as a fraction of the chord δ^*/c with and without transition strips, and of the transition location as a fraction of the chord x/c without transition strips.

CORRECTIONS

Corrections applied to the test data for the effects of the jet boundaries are based on equations presented in reference 2. The methods of reference 2 were extended in order that corrections to the flap hinge-moment coefficient and to the resultant balance-pressure coefficient might be obtained. The equations used in correcting the test data are as follows:

$$c_l = k_1 c_{l_u}$$

$$\alpha_o = \alpha_{o_u} + k_2 c_{l_{\delta_f=0^\circ}}$$

$$c_{h_f} = c_{h_{f_u}} + k_3 c_l$$

$$P_R = P_{R_u} + k_4 c_l$$

where the subscript u refers to the uncorrected value of the coefficient or angle, and the constants k_1, k_2, k_3, and k_4 depend on the test Mach number and have the following values for the conditions of the present tests:

M	k_1	k_2	k_3	k_4
0.20	0.966	0.221	0.0086	-0.0400
.34	.963	.231	.0094	-.0445
.40	.961	.238	.0099	-.0480

The corrections applied do not account for the effects of the boundary layers along the tunnel walls or for the effects of the small gaps between the ends of the flap and the end disks. The correction to the angle of attack does not account for the effect of the lift resulting from flap deflection. An estimate of the effect of the lift resulting from flap deflection indicated that, had this lift been accounted for, the values of the parameter c_{l_δ} would be about 1.5 percent smaller than the values of this parameter that are indicated by the data presented, and that the parameters c_{h_δ} and P_{R_δ} would be changed a negligible amount.

RESULTS AND DISCUSSION

Presentation of Data

Complete sets of data, including flap section hinge-moment coefficients, resultant balance-pressure coefficients, and airfoil section lift coefficients, were obtained for each of the flap contours shown in figure 1 for a Mach number of 0.34, with transition strips at 0.02c and the flap nose gap sealed. These data are presented in figures 4 to 9 as plots against flap deflection for various fixed angles of attack. Comparisons of the effects of fixed trailing-edge chord on various coefficients plotted against δ_f with $\alpha_o = 0^\circ$ and plotted against α_o with $\delta_f = 0^\circ$ are given in figures 10 to 19. Some additional tests were made to determine the effects on hinge-moment characteristics of Mach number (figs. 20 and 21), of transition strips (figs. 22 and 23), and of gap (figs. 24 and 25).

The measured parameter values at $\alpha_o = 0^\circ$ and $\delta_f = 0^\circ$, including slopes of the curves and incremental values of the coefficients resulting from surface-covering distortion, are given in table II. The data presented for resultant balance-pressure coefficients when used in conjunction with the hinge-moment data of plain flaps are useful in estimating the characteristics of sealed internally-balanced flaps.

An equation for calculating the hinge-moment coefficients of an internally-balanced flap is as follows (see reference 3):

$$c_{h_{\substack{\text{balanced}\\\text{flap}}}} = c_{h_{\substack{\text{plain}\\\text{flap}}}} + \frac{1}{2}P_R\left[\left(\frac{c_{bp}}{c_f}\right)^2\left(1 + m_s\right) - \left(\frac{t/2}{c_f}\right)^2\right] \qquad (1)$$

where m_s is the seal-moment ratio. Charts giving values of m_s for various balance-seal configurations are given in reference 3. For many configurations the term $\left(\frac{c_{bp}}{c_f}\right)^2\left(1 + m_s\right)$ may be replaced by $\left(\frac{c_b}{c_f}\right)^2$. Equation (1) then reduces to the form

$$c_{h_{\substack{\text{balanced}\\\text{flap}}}} = c_{h_{\substack{\text{plain}\\\text{flap}}}} + \frac{1}{2}P_R\left[\left(\frac{c_b}{c_f}\right)^2 - \left(\frac{t/2}{c_f}\right)^2\right] \qquad (2)$$

If it is assumed that the aerodynamic effects of distortion vary linearly with the amount of distortion, at least for amounts of distortion as large as that tested $(0.0233c_f)$, the results of this investigation can be made readily applicable to any amount of distortion up to $0.0233c_f$. On the basis of this assumption, values of incremental distortion parameters, defined as the incremental parameter values resulting from a maximum surface-covering distortion equal to one percent of the flap chord, were calculated from the test data. Because the tests included only fixed trailing-edge chords of $0.1c_f$ or more, estimates were made of the values of incremental distortion parameters for flaps with the distortion extending to the flap trailing edge. These values were estimated from unpublished correlations of data on the aerodynamic characteristics of control surfaces having various trailing-edge angles. Values of incremental distortion parameters obtained from the results of the present tests and by estimation are presented in table III. These values are strictly applicable only to the airfoil tested and cannot be assumed to apply exactly to any arbitrary airfoil section.

Effects of Fixed Trailing-Edge Chord

Hinge-moment characteristics.- The hinge-moment curves presented in figures 10 and 11 indicate that the primary effect of symmetrical distortion (contours CC and BB) is to rotate the hinge-moment curves, and thereby change the slope. For distortion that consists principally of a change in camber of the mean line (contours BF and BC) the primary effect on the hinge-moment curves is a displacement of the curves along the hinge-moment-coefficient axis with only small changes in the slopes.

The effects of fixed trailing-edge chord on the hinge-moment slopes c_{h_δ} and c_{h_α} are shown in figure 12. For symmetrical distortion, with the control surfaces concave, the hinge-moment parameters become less negative as the fixed trailing-edge chord is increased; and with the control surfaces bulged, the hinge-moment parameters become more negative as the fixed trailing-edge chord is increased. Even though the undistorted contour is maintained

over a part of the rear of the flap, the effect of symmetrical distortion is similar to the effect of variations in trailing-edge angle.

For all contours tested, the effects of distortion on the slopes c_{h_α} and c_{h_δ} decrease rapidly as the fixed trailing-edge chord is increased. The effects are almost entirely eliminated if the fixed trailing-edge chord is 30 percent of the flap chord.

The effects of surface-covering distortion on control forces depend on the displacement of the hinge-moment curves (camber effect) as well as on the slopes of the hinge-moment curves. The effect of fixed trailing-edge chord on the displacement of the hinge-moment curves (measured at $\alpha_o = 0^\circ$ and $\delta_f = 0^\circ$) is shown in figure 13. The displacement Δc_h is reduced quite rapidly as the fixed trailing-edge chord is increased, but it does not become negligible even with a fixed trailing-edge chord of 30 percent of the flap chord. The displacement of the hinge-moment curves is similar to that caused by a deflected tab on an undistorted flap and therefore will affect the control-surface characteristics accordingly.

Theoretical checks on the hinge-moment coefficient Δc_h at $\alpha_o = 0^\circ$ and $\delta_f = 0^\circ$ for contours BF and BC were obtained by assuming that the distorted contours could be replaced by multiply hinged flaps and by calculating the hinge moments according to the theory of reference 4. The comparison given in figure 13 indicates that, in general, the theory overestimates the effects of distortion by approximately 20 percent.

Resultant balance-pressure characteristics.- The curves of resultant balance-pressure coefficient plotted in figures 14 and 15 indicate that symmetrical distortions (contours BB and CC) have no appreciable effect on the resultant balance pressure. Camber distortion (contour BC) causes a displacement of the balance-pressure-coefficient curves.

The slopes P_{R_α} and P_{R_δ} are not greatly affected by variations of the flap contour. (See fig. 16.) Figure 16 also shows that the displacement ΔP_R of the balance-pressure coefficient at $\alpha_o = 0^\circ$ and $\delta_f = 0^\circ$ is approximately constant regardless of the fixed trailing-edge chord. This constancy seems to indicate that the value of ΔP_R depends primarily on the flap contour near the flap hinge and is not affected to any great extent by the flap

contour near the trailing edge. For the flaps tested in this investigation, the distortion began at a distance $0.067c_f$ to the rear of the flap hinge line. Had the distortion begun at or very near the flap hinge line, the effect of distortion on ΔP_R probably would have been considerably greater than that obtained.

In order to illustrate the effect of camber distortion on the hinge moments of sealed internally-balanced flaps, equation (2) may be rewritten in terms of incremental, rather than absolute, values of hinge-moment and resultant balance-pressure coefficients, which gives

$$\Delta c_{h_{\substack{\text{balanced}\\\text{flap}}}} = \Delta c_{h_{\substack{\text{plain}\\\text{flap}}}} + \frac{1}{2}\Delta P_R\left[\left(\frac{c_b}{c_f}\right)^2 - \left(\frac{t/2}{c_f}\right)^2\right]$$

Since camber distortion results in increments Δc_h and ΔP_R that are of the same sign (see figs. 13 and 16), the increment Δc_h of a balanced flap is larger than the increment Δc_h of a plain or unbalanced flap. The effect of camber distortion on flap hinge-moment characteristics, therefore, would be expected to increase somewhat as the balance chord c_b is increased.

Lift characteristics.- Curves of lift coefficient plotted in figures 17 and 18 indicate that neither camber nor symmetrical distortion has any appreciable effect on lift characteristics. Figure 19 shows that the slopes c_{l_α} and c_{l_δ} are almost unaltered by the fixed trailing-edge chord and that the increment of lift Δc_l caused by camber distortion is small and decreases with increase in fixed trailing-edge chord.

Values of Δc_l calculated by the theory of multiply hinged flaps (reference 4) are included in figure 19 for comparison with the experimental values of Δc_l.

Effect of Mach Number

The results of the present tests indicated that if the fixed trailing-edge chord were 20 percent of the flap chord most of the parameters of the airfoil and flap would be nearly independent of

control-surface distortion. Tests, therefore, were made to determine whether the hinge-moment characteristics of the distorted flaps having values of $\frac{c_\phi}{c_f} = 0.20$ would be affected by Mach number more adversely than the hinge-moment characteristics of the undistorted flap.

As shown in figures 20 and 21, Mach number variations within the speed range tested have very small effects either on the characteristics of the distorted flaps with $\frac{c_\phi}{c_f} = 0.20$ or on the characteristics of the undistorted flap.

Effects of Transition Strips

The effects of transition strips on flap section hinge-moment coefficient plotted against flap deflection (fig. 22) and against angle of attack (fig. 23) were determined for the undistorted flap contour and for various distorted flap contours having values of $\frac{c_\phi}{c_f} = 0.20$. Figures 22 and 23 show that removing the transition strips makes the slope c_{h_δ} more negative over a δ_f range of approximately $\pm 6^\circ$ and makes the slope c_{h_α} more negative over an α_o range of approximately $\pm 1^\circ$. At the limits of these ranges the hinge-moment curves of the model without transition strips show an abrupt change in slope resulting from a shift in transition point from a rearward to a forward position. Similar results have been observed in other tunnels having a low turbulence level (of the order of that of the tunnel used for the present tests). The effects of the strips on the slopes of the hinge-moment curves are largest for contour BB and smallest for contour CC. Several investigations of beveled flaps made in both the United States and Great Britain have indicated that the incremental changes in hinge moments resulting from the addition of strips are roughly proportional to the trailing-edge angle. Although the trailing-edge angle was maintained constant over a chord length $c_\phi = 0.20c_f$ for the flaps of this investigation, the characteristics obtained with contour BB are similar to the characteristics that would be expected with a large trailing-edge angle and the characteristics obtained with contour CC are similar to the characteristics that would be expected with a small trailing-edge angle. In general, if the flap contour

tends to bulge, boundary-layer effects may be large (as indicated by the effects of strips) even though a relatively small trailing-edge angle is maintained over at least 20 percent of the flap chord.

Effects of Gap

Comparisons of the effects of gap are given for the undistorted flap contour and for the distorted flap contours having $\frac{c_\phi}{c_f} = 0.20$ in figures 24 and 25. When the distortion consists of an increase in the thickness of the control surface (an effective increase in trailing-edge angle), opening the gap causes c_{h_α} and c_{h_δ} to become less negative; and when the distortion consists of a decrease in thickness of the control surface (an effective decrease in trailing-edge angle), opening the gap usually causes c_{h_α} and c_{h_δ} to become more negative. These results agree qualitatively with results given in reference 5, which show similar variations in the effect of gap with variations in the actual trailing-edge angle.

Application of Data to an Assumed Airplane

In order to illustrate the possible benefits of maintaining the undistorted contour over a part of the chord of a control surface, the experimental results obtained in this investigation have been applied to an assumed fighter-type airplane having the following characteristics:

Ratio of stick force to elevator moment, K	0.60
Wing loading, W/S_w, pounds per square foot	40.0
Dynamic pressure ratio, q_t/q	1.0
Wing lift-curve slope, $\left(C_{L_\alpha}\right)_w$	.072
Horizontal-tail incidence, i_t, degrees	0
Ratio of horizontal-tail area to wing area, S_t/S_w	.20
Ratio of tail length to wing mean aerodynamic chord, l/c'	4.0
Elevator lift-curve slope, C_{L_δ}	.033
Elevator size factor, $b_e\bar{c}_e^2$, cubic feet	20.0
Airplane stability factor, x'/c'	-.05
Wing aspect ratio, A_w	6.0
Horizontal-tail aspect ratio, A_t	3.0
Downwash angle factor, $1 - \frac{\partial \epsilon}{\partial \alpha}$	0.40

Calculations have been made of the stick-force increments resulting from elevator surface-covering distortion that are required to hold the airplane in level flight at a given speed. The amount and the type of distortion of the elevator of a specific airplane will, of course, vary with speed; and therefore, the curve of stick force plotted against speed for a given setting of the trimming device may vary between limits determined by the characteristics of the control surface with maximum fixed amounts of distortion. The increments of stick force (at a given speed) corresponding to a constant amount of distortion for each of the contours considered in this investigation is indicative of the maximum change in stick force for the amount and type of distortion assumed and therefore may be used as a basis for comparing the effects of the various kinds of distortion. These stick-force increments would not have to be supplied by the pilot of an airplane equipped with a trimming device, but they are roughly proportional to the deflection of the trimming device that is required to offset the effects of surface-covering distortion. The following equation, which is based on linear slopes, was used in making the calculations:

$$\Delta F = \left\{ \left[\frac{\left(\frac{W}{S_w}\right)\left(\frac{q_t}{q}\right)\left(1 - \frac{\partial \epsilon}{\partial \alpha}\right)}{\left(C_{L_\alpha}\right)_w} + q_t i_t \right] \Delta C_{h_\alpha} + \left[\frac{\left(\frac{W}{S_w}\right)\left(\frac{x'}{c'}\right)}{\left(\frac{S_t}{S_w}\right)\left(\frac{l}{c'}\right) C_{L_\delta}} \right] \Delta C_{h_\delta} - \frac{q_t \, \Delta C_L \left(C_{h_\delta}\right)_{\text{distorted}}}{C_{L_\delta}} + q_t \, \Delta C_h \right\} K b_e \bar{c}_e^{\,2} \qquad (3)$$

in which $\left(C_{L_\alpha}\right)_w$ is the lift-curve slope of the airplane wing; all other parameters are for the horizontal tail. Equation (3) accounts for the effects of elevator distortion on C_{h_α}, C_{h_δ}, ΔC_h of the plain elevator, ΔP_R, and ΔC_L but neglects the very small effects of distortion on P_{R_α}, P_{R_δ}, C_{L_α}, and C_{L_δ}. All calculations for the distorted contours were made for the condition of maximum distortions of one percent of the elevator chord. The values of the

incremental distortion parameters given in table III therefore represent the total aerodynamic effects of the amount of distortion assumed. The section parameters given in table III were converted to finite-span parameters for use in equation (3) by means of the aspect-ratio-correction formulas given in reference 6. Calculations were made for plain sealed elevators and for sealed internally balanced elevators having a balance-chord ratio $\frac{c_b}{c_f} = 0.40$. A calibrated airspeed of 300 miles per hour was assumed.

The results of the calculations are presented in figure 26. Stick-force increments for $\frac{c_d}{c_e} = 0$ were calculated from the estimated incremental distortion parameters given in table III. For the assumed conditions the effects of symmetrical distortion are very small when compared with the effects of camber distortion. Variations in the constants of the assumed airplane would affect the relative importance of the two kinds of distortion, but for almost any airplane configuration a given amount of camber distortion can be expected to be much more important than the same amount of symmetrical distortion. Figure 26 shows that the effects of symmetrical distortion are largely eliminated by maintaining the undistorted contour over the rear 20 percent of the elevator chord. When the distortion involves a change in camber, approximately 75 percent of the effects of distortion are eliminated by maintaining the undistorted contour over the rear 20 percent of the elevator chord and approximately 83 percent of the effects of distortion are eliminated by maintaining the undistorted contour over the rear 30 percent of the elevator chord. Although these percentage values were obtained from calculations of the effects of distortion on stick forces in level flight, approximately the same percentage values would be expected to apply to the effects of distortion on the stick forces in accelerated maneuvers.

Figure 26 shows that, except for the elevator having maximum camber distortion (contour BC), the effects of distortion are approximately the same either for the plain elevator or for the elevator with an internal-balance-chord ratio $\frac{c_b}{c_e} = 0.40$. For contour BC the effects of distortion were greater for the balanced elevator than for the plain elevator. As pointed out previously, the balance might have had a considerably more adverse effect had the distortion occurred very close to the elevator hinge line, rather than at a distance $0.067c_e$ behind the hinge line.

Although the analysis presented herein has been made specifically for an elevator control, the conclusions concerning the reductions in distortion effects that are made possible by maintaining the undistorted contour over a part of the control-surface chord are believed to apply to rudder and aileron controls, as well.

CONCLUSIONS

The present investigation of a modified NACA 65_1-012 airfoil having a 30-percent airfoil-chord flap with contours simulating various distorted surface-covering shapes indicates the following conclusions:

1. The effects of surface-covering distortion on lift characteristics generally are small when compared with the effects of surface-covering distortion on hinge-moment characteristics.

2. Approximately 75 percent of the effects of distortion on stick forces can be eliminated by maintaining the undistorted flap contour over the rear 20 percent of the flap chord.

3. When the flap has been thickened by distortion, opening the gap at the flap nose or placing transition strips near the airfoil leading edge generally causes the variations of hinge-moment coefficient with angle of attack and with flap deflection to become less negative. Opening the gap generally has the opposite effect if distortion consists of a decrease in flap thickness.

4. Variations in Mach number from 0.20 to 0.40 have only small effects on the hinge-moment characteristics of the undistorted flap or the distorted flaps having the undistorted contour maintained over the rear 20 percent of the flap chord.

Langley Memorial Aeronautical Laboratory
National Advisory Committee for Aeronautics
Langley Field, Va., February 11, 1947

REFERENCES

1. Mathews, Charles W.: An Analytical Investigation of the Effects of Elevator-Fabric Distortion on the Longitudinal Stability and Control of an Airplane. NACA ACR No. L4E30, 1944.

2. Allen, H. Julian, and Vincenti, Walter G.: Wall Interference in a Two-Dimensional-Flow Wind Tunnel with Consideration of the Effect of Compressibility. NACA ARR No. 4K03, 1944.

3. Fischel, Jack: Hinge Moments of Sealed-Internal-Balance Arrangements for Control Surfaces. II - Experimental Investigation of Fabric Seals in the Presence of a Thin-Plate Overhang. NACA ARR No. L5F30a, 1945.

4. Perring, W. G. A.: The Theoretical Relationships for an Aerofoil with a Multiply Hinged Flap System. R. & M. No. 1171, British A.R.C., 1928.

5. Hoggard, H. Page, Jr., and Bullock, Marjorie E.: Wind-Tunnel Investigation of Control-Surface Characteristics. XVI - Pressure Distribution over an NACA 0009 Airfoil with 0.30-Airfoil-Chord Beveled-Trailing-Edge Flaps. NACA ARR No. L4D03, 1944.

6. Swanson, Robert S., and Crandall, Stewart M.: Lifting-Surface-Theory Aspect-Ratio Corrections to the Lift and Hinge-Moment Parameters for Full-Span Elevators on Horizontal Tail Surfaces. NACA TN No. 1175, 1947.

TABLE I.- ORDINATES FOR MODIFIED NACA 65_1-012 AIRFOIL

[Stations and ordinates in percent of airfoil chord]

Station	Ordinate
0	0
1.25	1.39
2.50	1.88
5.00	2.60
7.50	3.17
10.00	3.65
15.00	4.40
20.00	4.97
25.00	5.40
30.00	5.72
40.00	6.00
50.00	5.76
60.00	4.94
70.00	3.74
75.00	3.14
80.00	2.53
85.00	1.92
90.00	1.31
95.00	0.72
100.00	0.10
Leading-edge radius:	1.000 percent c

TABLE II.- PARAMETER VALUES FOR 0.30C FLAPS ON A MODIFIED NACA 65_1-012 AIRFOIL

[Values measured at $\alpha_o = 0°$; $\delta_f = 0°$]

Flap contour	$\frac{c_f'}{c_f}$	Gap	Position of transition strips	Mach number M	c_{l_α}	c_{l_δ}	c_{h_α}	c_{h_δ}	P_{R_α}	P_{R_δ}	Δc_l (a)	Δc_h (a)	ΔP_R (a)
FF	1.0	Sealed	.02c	0.20	-----	-----	-0.0032	-0.0089	-----	-----	-----	0	0
↓	↓	↓	↓	.34	0.103	0.062	-.0031	-.0089	0.036	0.096	0	0	0
				.40	-----	-----	-.0027	-.0089	-----	-----	-----	0	0
		Off	Off	.34	-----	.067	-.0058	-.0110	-----	-----	0	0	0
↓	↓	.005c	.02c	.34	-----	-----	-.0018	-.0079	-----	-----	-----	0	------
CC	0.1	Sealed	.02c	.34	.103	.064	-.0052	-.0103	.035	.097	0	0	0
	0.2			.20	-----	-----	-.0042	-.0089	-----	-----	-----	0	------
				.34	.103	.064	-.0040	-.0093	.036	.098	0	0	0
				.40	-----	-----	-.0040	-.0093	-----	-----	-----	0	------
		Off	Off	.34	-----	.069	-.0045	-.0108	-----	-----	0	0	0
		.005c	.02c	.34	-----	-----	-.0058	-.0119	-----	-----	-----	0	------
↓	0.3	Sealed	.02c	.34	.103	.064	-.0031	-.0091	.035	.097	0	0	0
HB	0.1	Sealed	.02c	.34	.103	.057	0.0000	-.0065	.037	.090	0	0	0
	0.2			.20	-----	-----	-.0024	-.0077	-----	-----	-----	0	------
				.34	.103	.058	-.0021	-.0082	.037	.090	0	0	0
				.40	-----	-----	-.0018	-.0082	-----	-----	-----	0	------
		Off	Off	.34	-----	.068	-.0058	-.0116	-----	-----	0	0	------
		.005c	.02c	.34	-----	-----	-.0007	-.0055	-----	-----	-----	0	------
↓	0.3	Sealed	.02c	.34	.103	.059	-.0028	-.0088	.037	.090	0	0	0
FC	0.1	Sealed	.02c	.34	-----	.064	-.0041	-.0094	-----	.097	.025	-.028	-.035
↓	0.2	↓	↓	↓	-----	.062	-.0038	-.0092	-----	.096	.010	-.020	-.050
	0.3				-----	.062	-.0033	-.0090	-----	.094	.010	-.009	-.050
EF	0.1	Sealed	.02c	.34	-----	.058	-.0019	-.0077	-----	.093	.030	-.032	-.053
↓	0.2	↓	↓	↓	-----	.060	-.0029	-.0086	-----	.093	.035	-.020	-.045
	0.3				-----	.060	-.0034	-.0088	-----	.092	.020	-.015	-.070
BC	0.1	Sealed	.02c	.34	.103	.061	-.0034	-.0096	.037	.092	.045	-.058	-.110
	0.2			.20	-----	-----	-.0044	-.0090	-----	-----	-----	-.039	-.110
				.34	.103	.061	-.0037	-.0090	.036	.090	.025	-.038	-.100
				.40	-----	-----	-.0033	-.0090	-----	-----	-----	-.039	------
		Off	Off	.34	-----	.068	-.0050	-.0114	-----	-----	.030	-.039	------
		.005c	.02c	↓	-----	-----	-.0051	-.0097	-----	-----	-----	-.044	------
↓	0.3	Sealed	.02c		.103	.061	-.0032	-.0088	.036	.090	.025	-.022	-.100

[a] Assumed to be zero for all symmetric contours.

TABLE III.- INCREMENTAL DISTORTION PARAMETER VALUES FOR 0.30C FLAPS ON MODIFIED NACA 65_1-012 AIRFOIL

[Values measured at $\alpha_o = 0^\circ$, $\delta_f = 0^\circ$. Gap sealed; transition strips at 0.02C; M = 0.34]

Flap contour	$\frac{o_f}{c_f}$	$\Delta c_{l_\alpha}'$	$\Delta c_{l_\delta}'$	$\Delta c_{h_\alpha}'$	$\Delta c_{h_\delta}'$	$\Delta P_{R_\alpha}'$	$\Delta P_{R_\delta}'$	$\Delta c_l'$	$\Delta c_h'$	$\Delta P_R'$
FF	1.0	0	0	0	0	0	0	0	0	0
CC	0	-----	------	[a]-0.0015	[a]-0.0079	-------	------	0	0	0
↓	.10	0	0.0009	-.00090	-.00060	-0.0004	0.0004	0	0	0
	.20	0	.0009	-.00039	-.00017	0	.0009	0	0	0
	.30	0	.0009	0	-.00009	-.0017	.0004	0	0	0
EB	0	-	------	[a].0027	[a].0017	-------	------	0	0	0
↓	.10	0	-.0022	.00133	.00103	.0004	-.0026	0	0	0
	.20	0	-.0017	.00043	.00047	.0004	-.0026	0	0	0
	.30	0	-.0013	.00013	.00004	.0004	-.0026	0	0	0
FC	0	-	------	[a]-.0007	[a]-.0003	-------	------	[a].0378	[a]-.0326	------
↓	.10	0	.0009	-.00043	-.00022	.0004	.0004	.0107	-.0120	-.0150
	.20	0	0	-.00030	-.00013	.0008	0	.0043	-.0086	-.0215
	.30	0	0	-.00009	-.00004	.0008	-.0009	.0043	-.0039	-.0215
EF	0	-	------	[a].0010	[a].0011	-------	------	[a].0403	[a]-.0348	------
↓	.10	0	-.0017	.00052	.00052	.0004	-.0013	.0129	-.0137	-.0227
	.20	0	-.0009	.00009	.00013	.0008	-.0013	.0150	-.0086	-.0193
	.30	0	-.0009	-.00013	.00004	.0008	-.0017	.0086	-.0064	-.0300
BC	0	-	------	[a]-.0011	[a]-.0009	-------	------	[a].0670	[a]-.0601	------
↓	.10	0	-.0004	-.00013	-.00030	.0004	-.0017	.0193	-.0249	-.0472
	.20	0	-.0004	-.00026	-.00004	0	-.0026	.0107	-.0163	-.0429
	.30	0	-.0004	-.00004	-.00004	0	-.0026	.0107	-.0094	-.0429

[a]Estimated values.

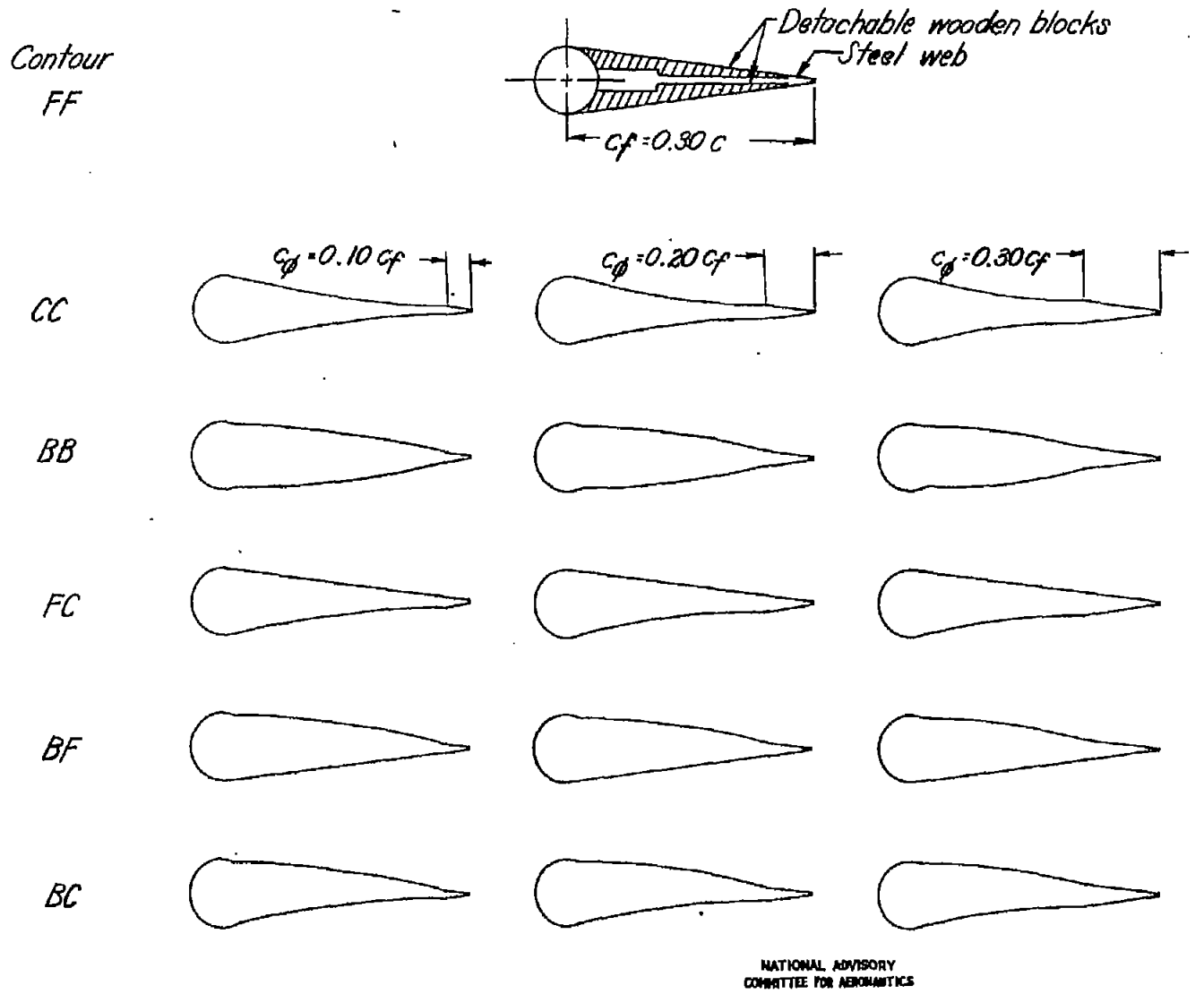

Figure 1.- Contours of the various 0.30c plain flaps used on the modified NACA 65_1-012 airfoil.

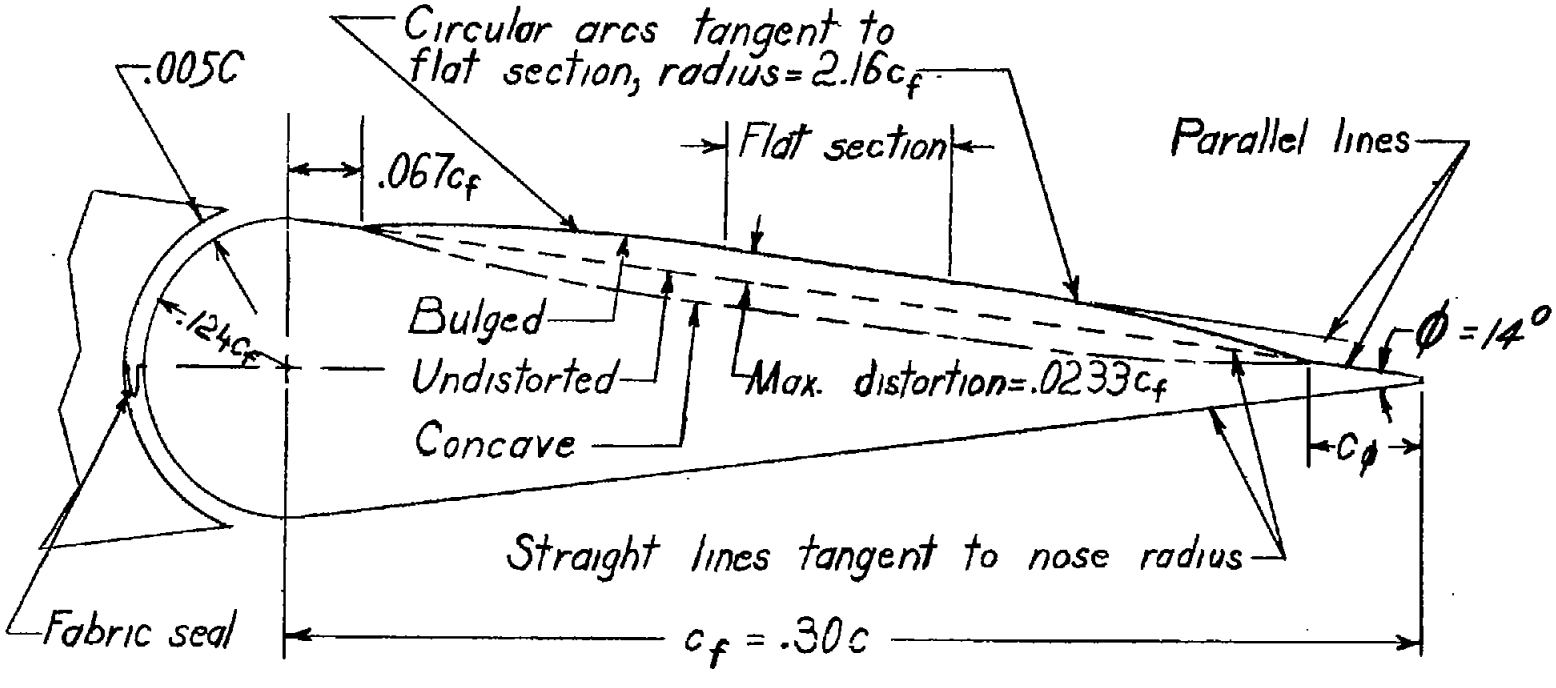

c_ϕ/c_f	Length of flat section
0.1	$0.2c_f$
0.2	$0.1c_f$
0.3	0

NATIONAL ADVISORY COMMITTEE FOR AERONAUTICS

Figure 2.- Construction of contours for the 0.30c plain flaps used on the modified NACA 65_1-012 airfoil.

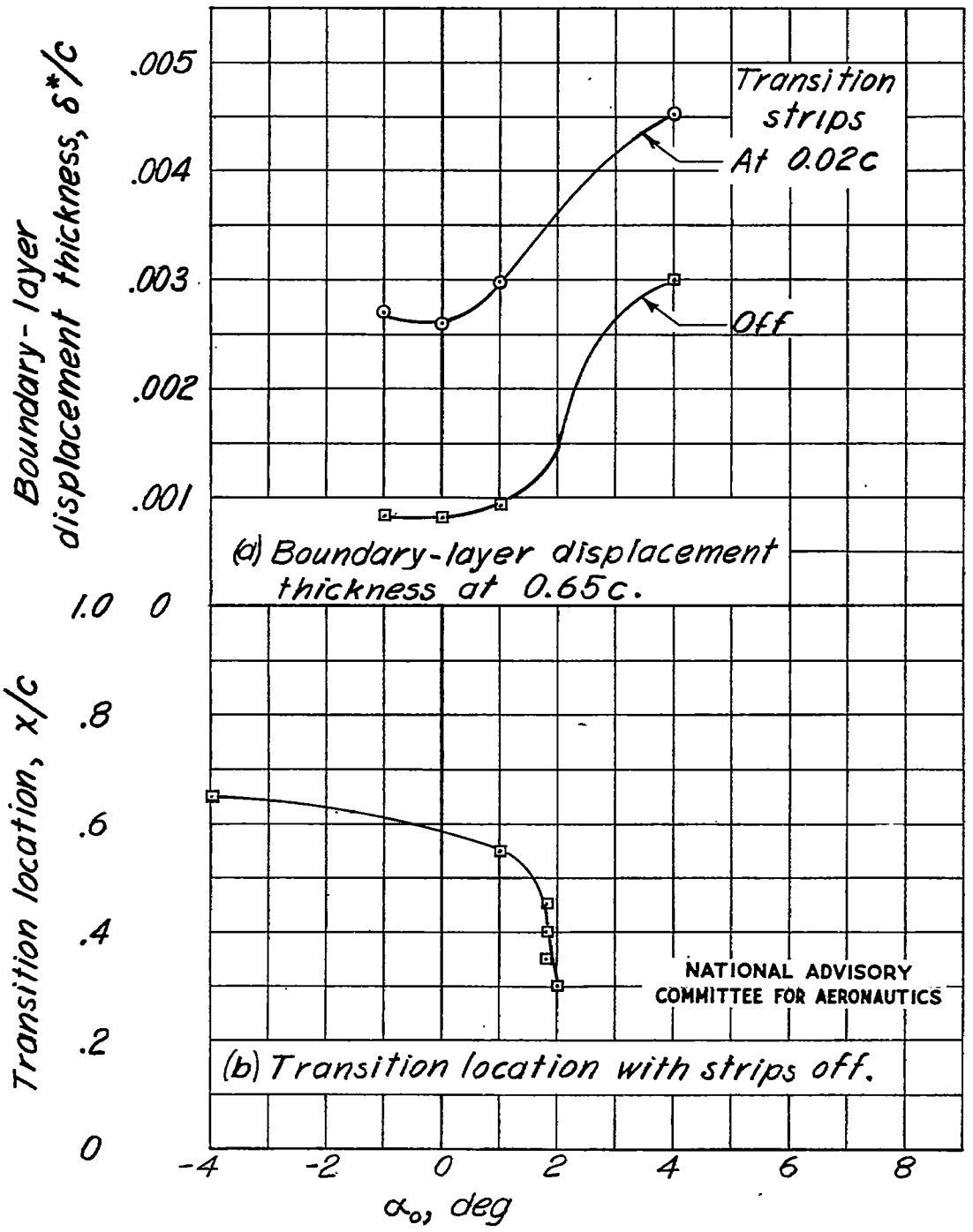

Figure 3.- Boundary-layer characteristics on upper surface of modified NACA 65_1-012 airfoil. Flap contour, FF; gap sealed; M, 0.34.

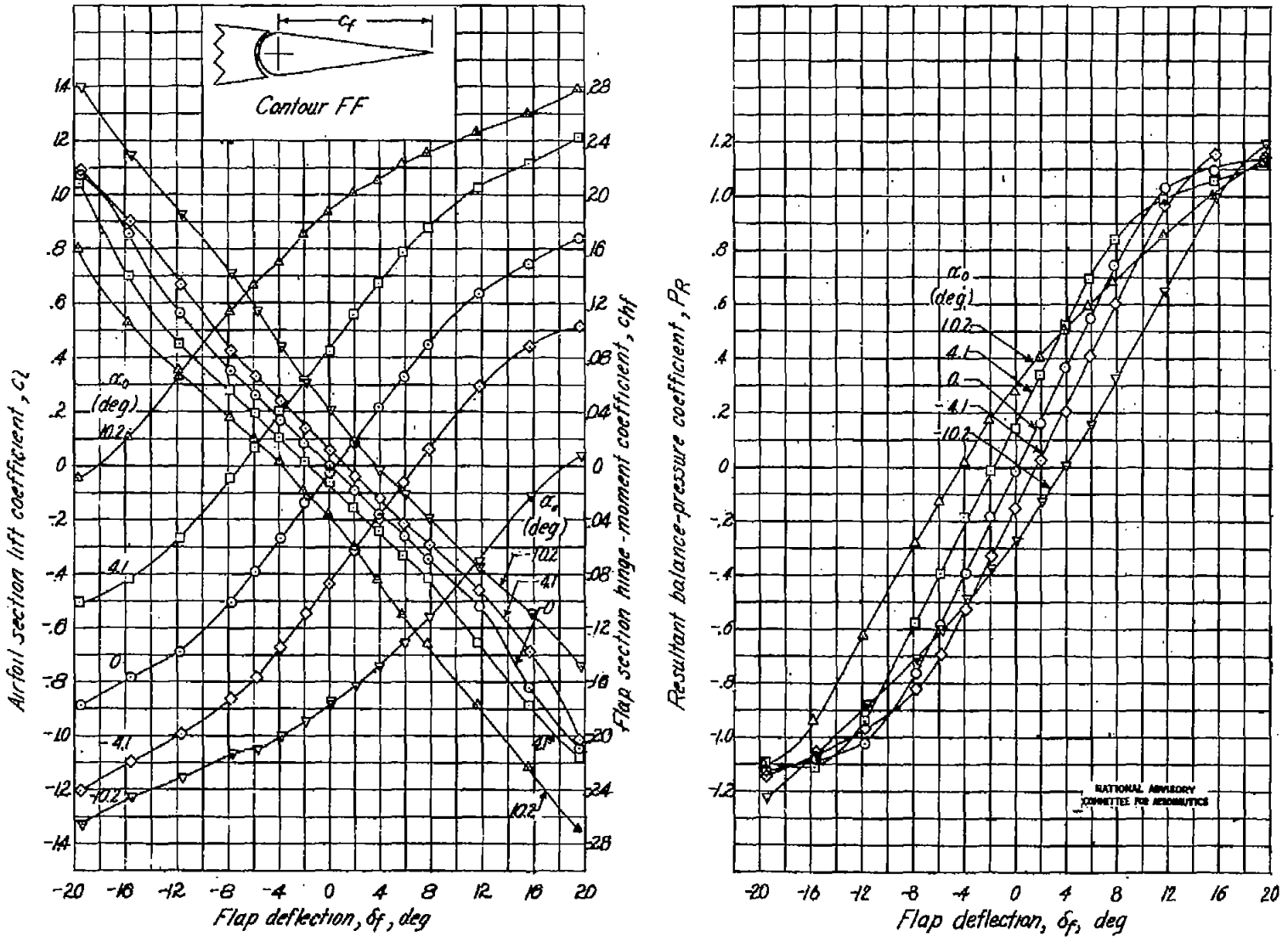

Figure 4.- Section aerodynamic characteristics of modified NACA 65_1-012 airfoil with 0.30c flap. Flap contour FF; gap sealed; transition strips at 0.02c; M, 0.34.

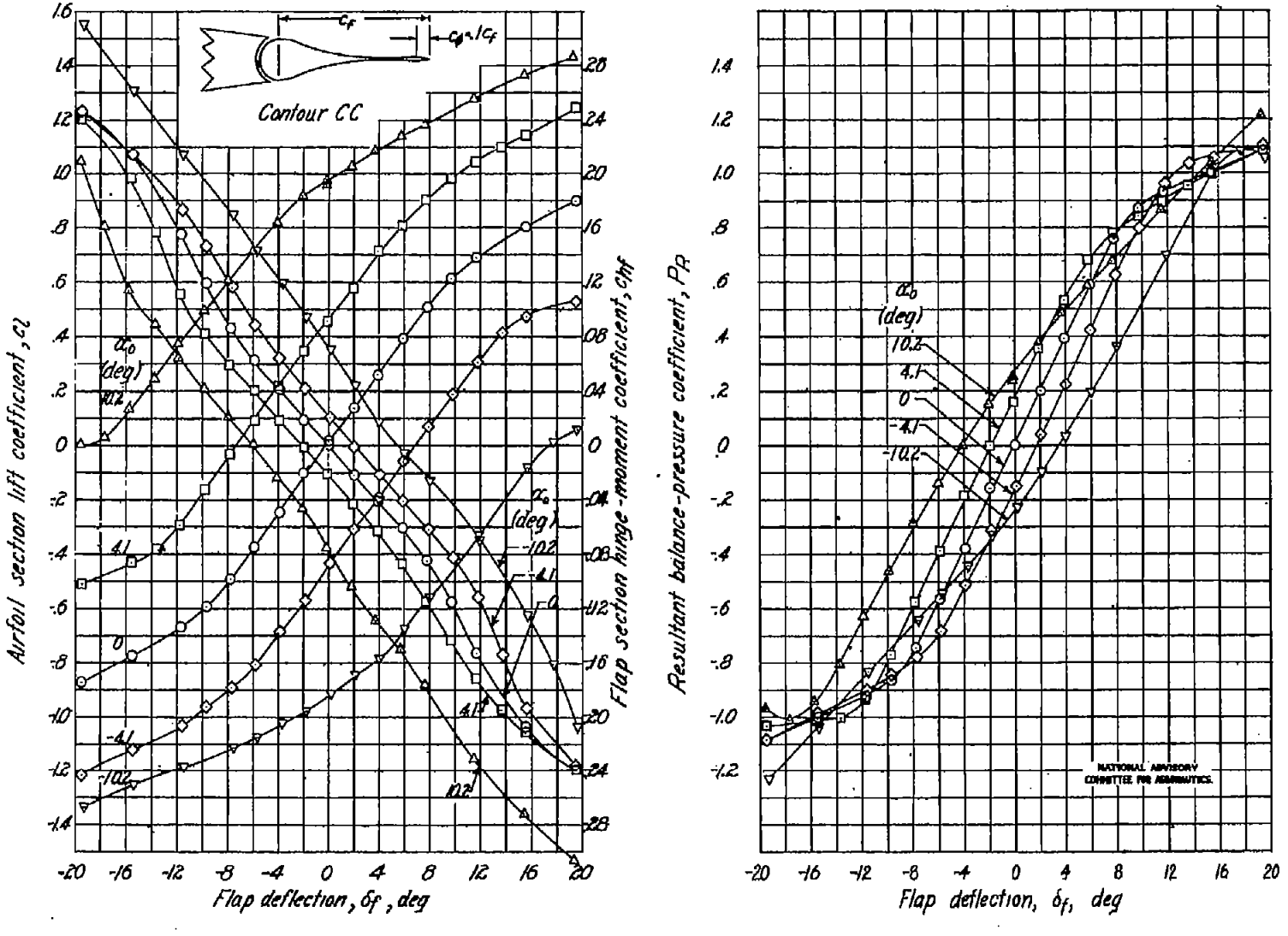

(a) $\frac{c_g}{c_f} = 0.1$.

Figure 5.- Section aerodynamic characteristics of modified NACA 65_1-012 airfoil with 0.30c flap. Flap contour CC; gap sealed; transition strips at 0.02c; M, 0.34.

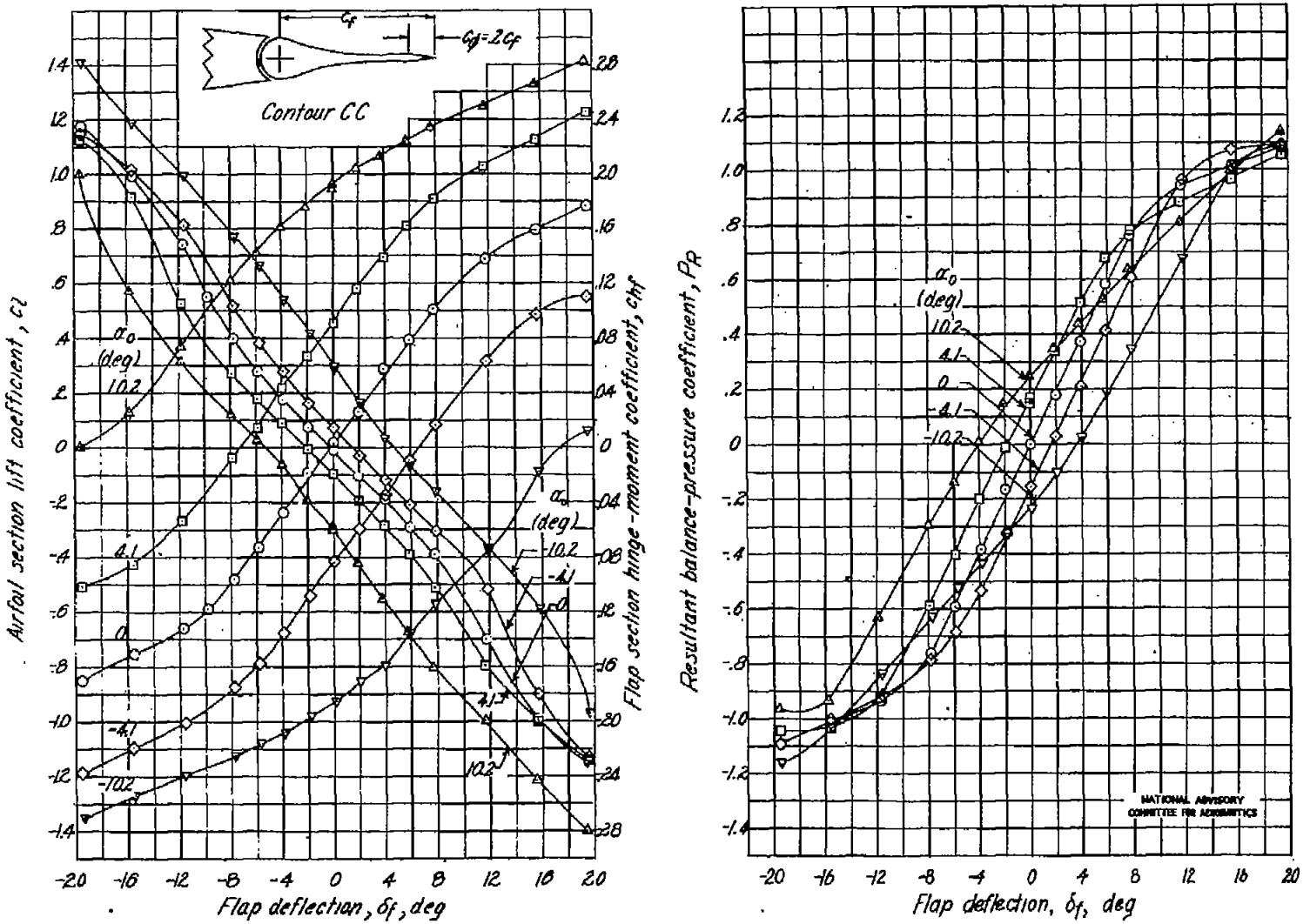

(b) $\frac{c_\phi}{c_f} = 0.2$.

Figure 5.- Continued.

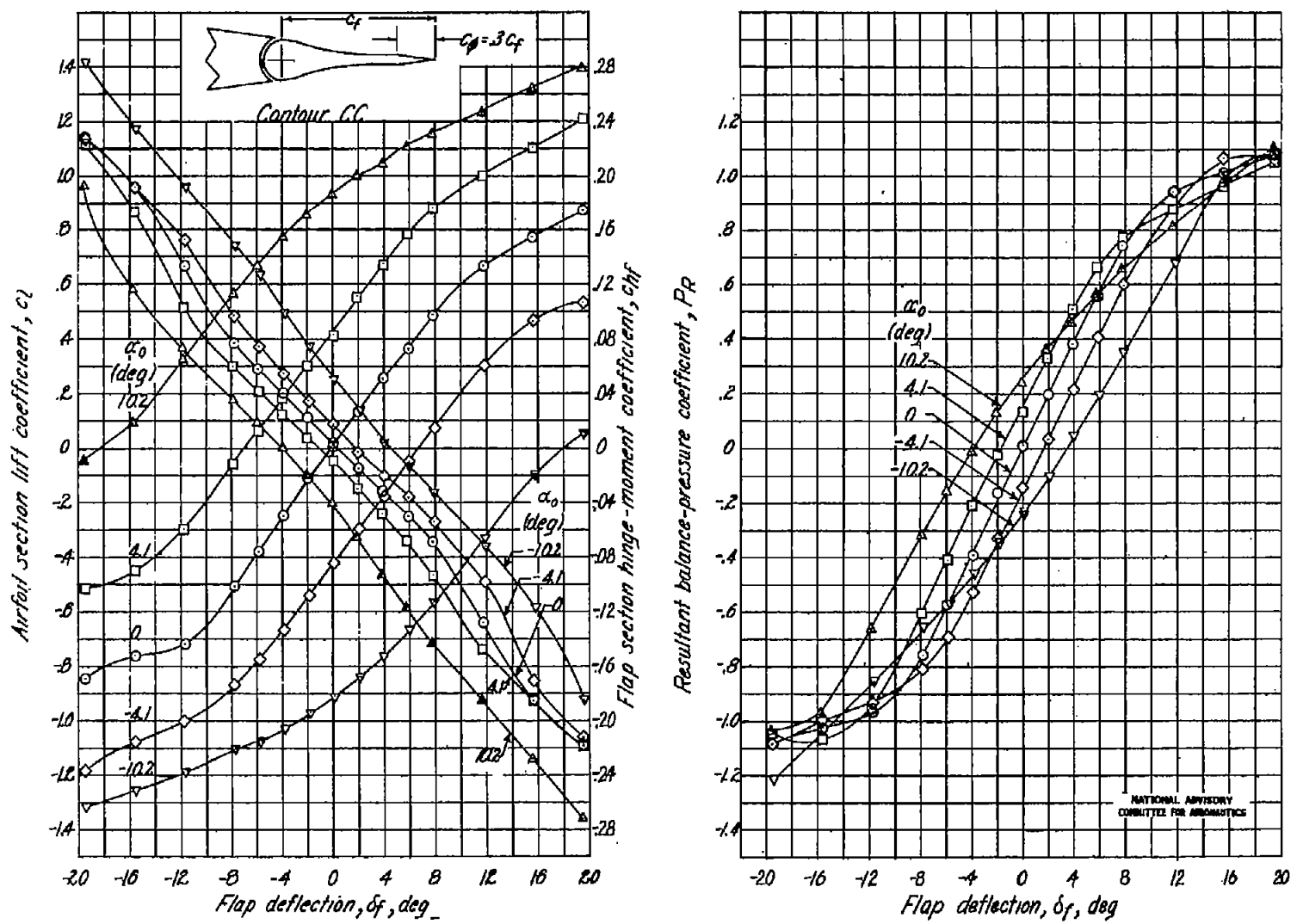

(c) $\frac{c_\phi}{c_f} = 0.3$.

Figure 5.- Concluded.

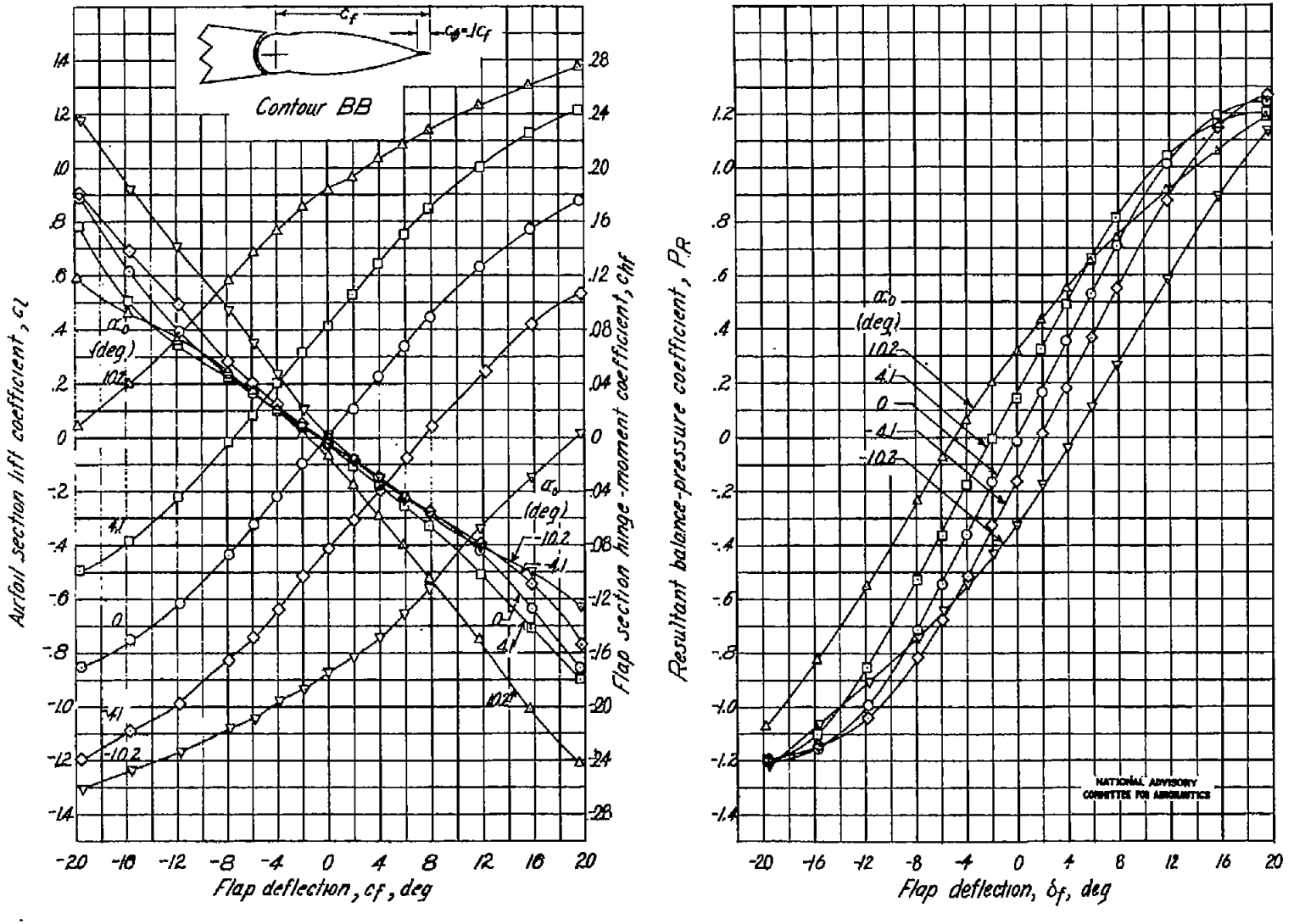

(a) $\frac{c_\phi}{c_f} = 0.1$.

Figure 6.- Section aerodynamic characteristics of modified NACA 65_1-012 airfoil with 0.30c flap. Flap contour BB; gap sealed; transition strips at 0.02c; M, 0.34.

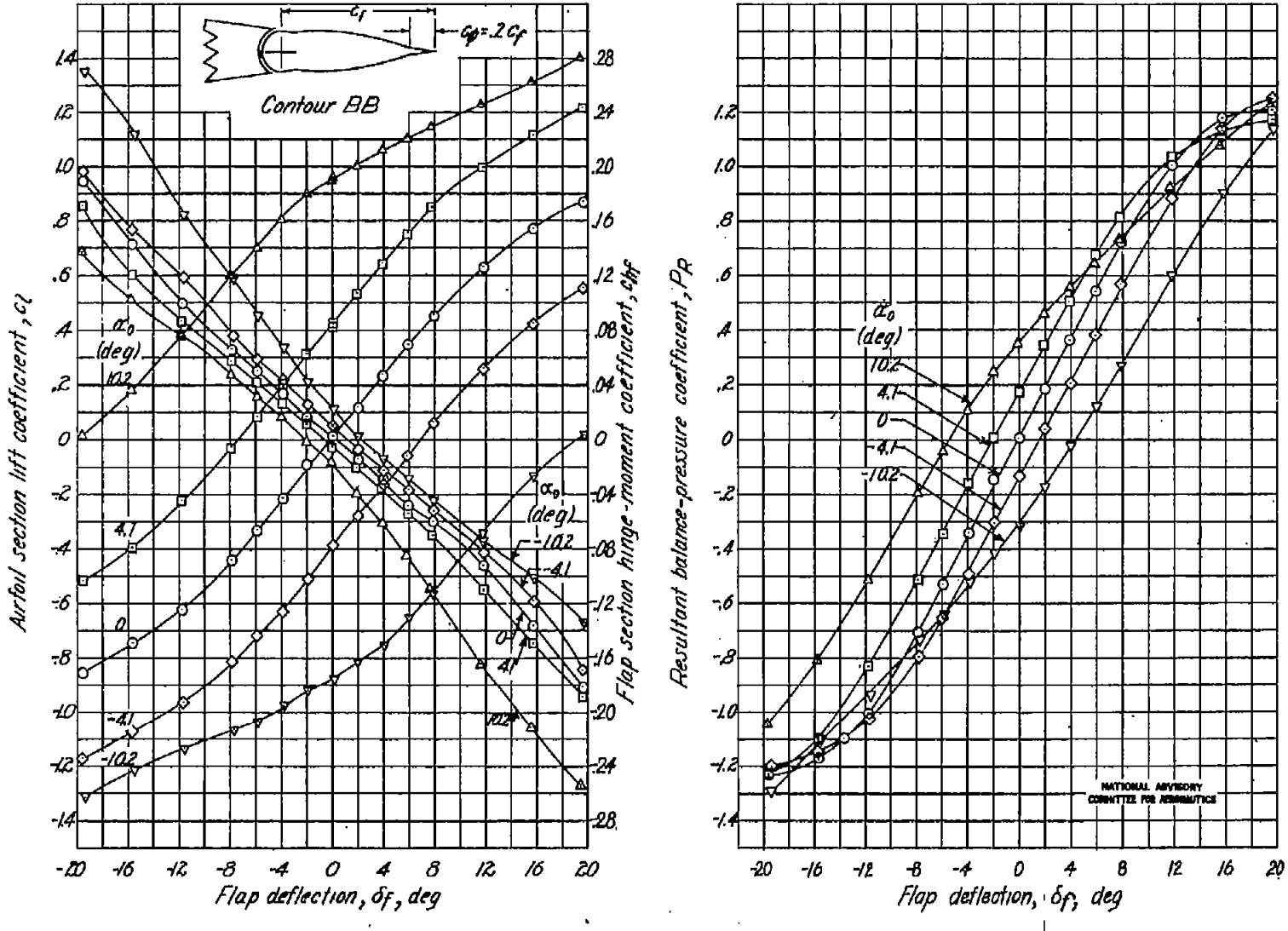

(b) $\frac{c_\phi}{c_f} = 0.2$.

Figure 6.- Continued.

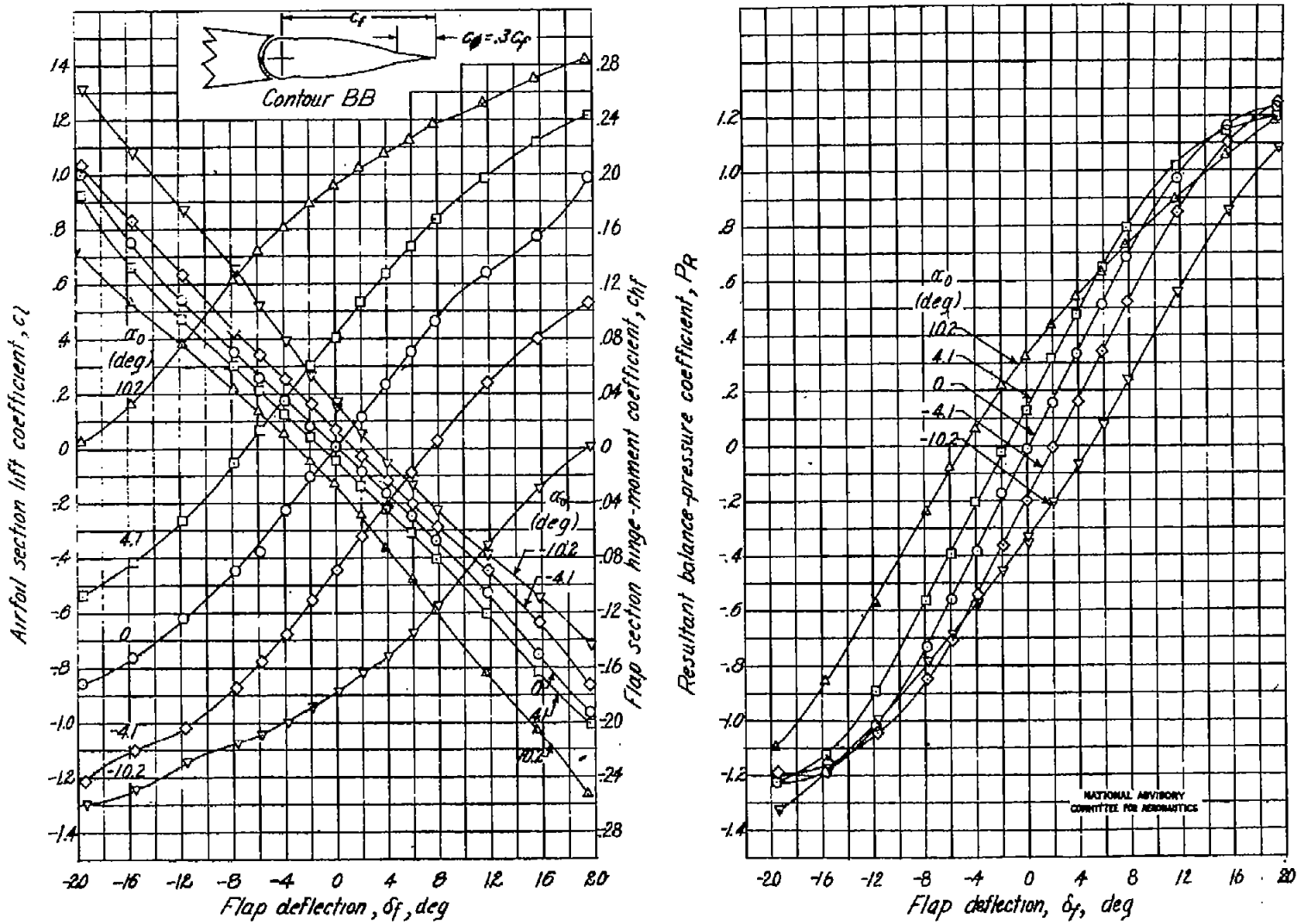

(c) $\frac{c_\phi}{c_f} = 0.3$.

Figure 6.- Concluded.

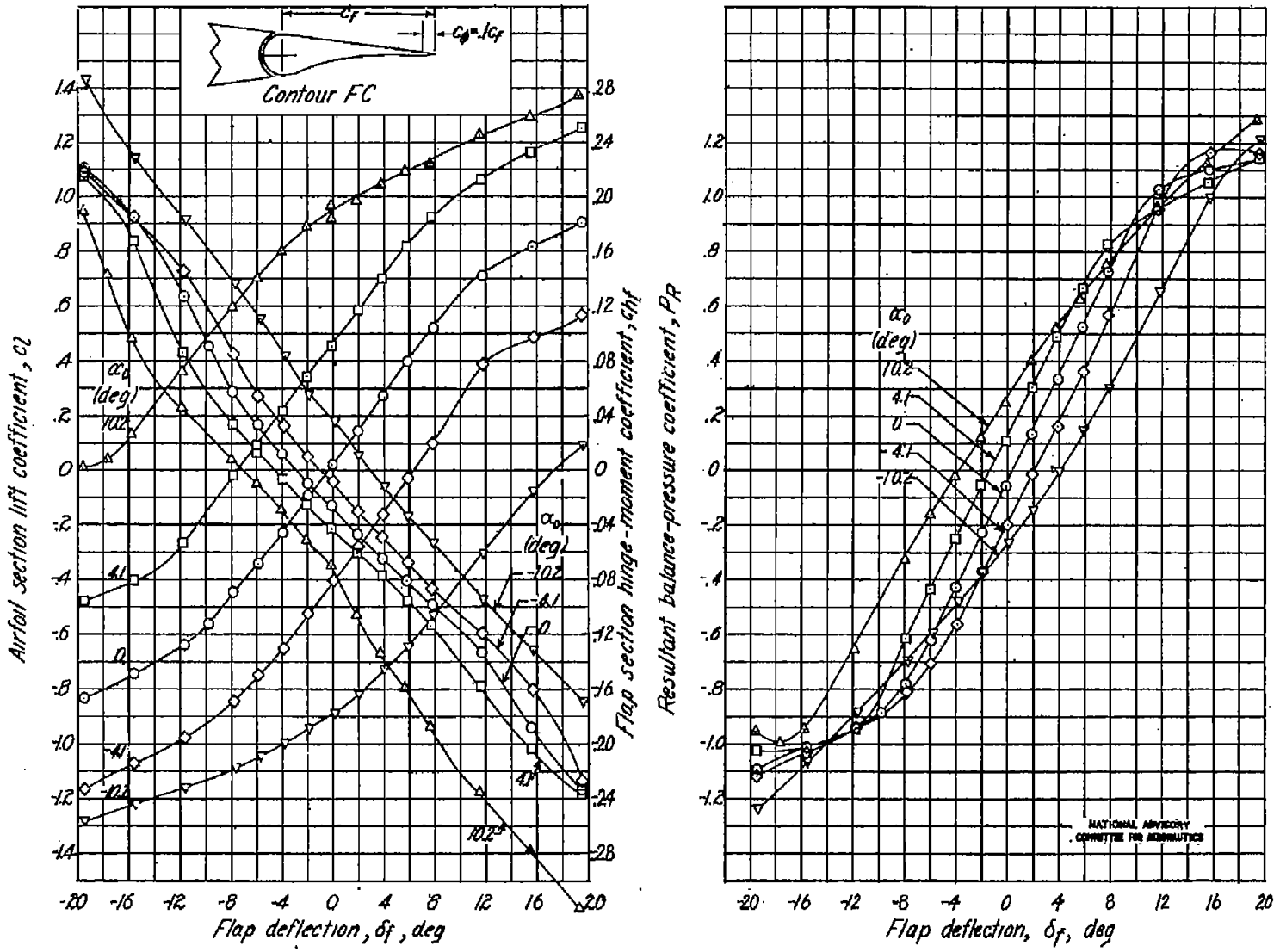

(a) $\frac{c_\phi}{c_f} = 0.1$.

Figure 7.- Section aerodynamic characteristics of modified NACA 65_1-012 airfoil with 0.30c flap. Flap contour FC; gap sealed; transition strips at 0.02c; M, 0.34.

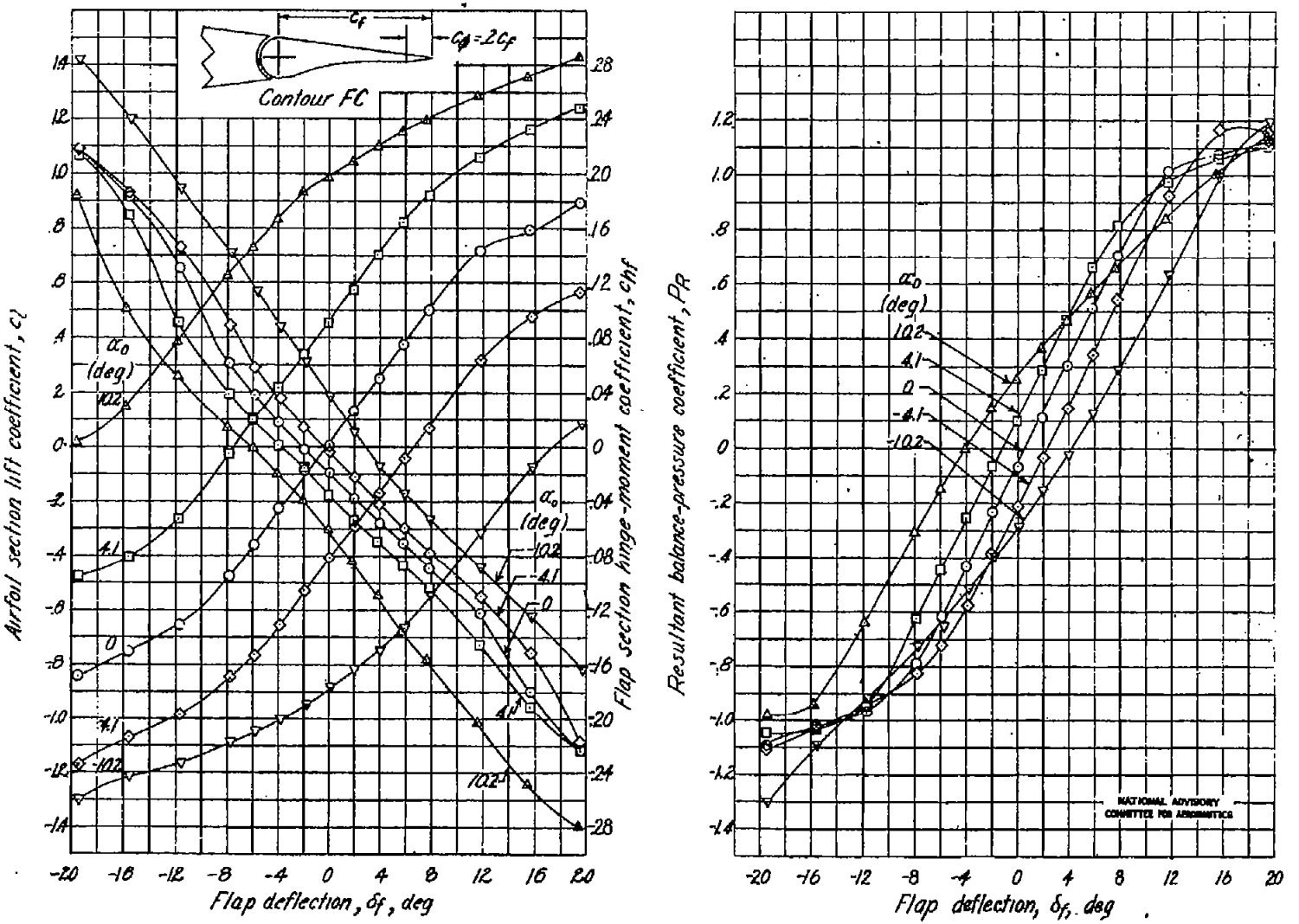

(b) $\frac{c_\phi}{c_f} = 0.2$.

Figure 7.- Continued.

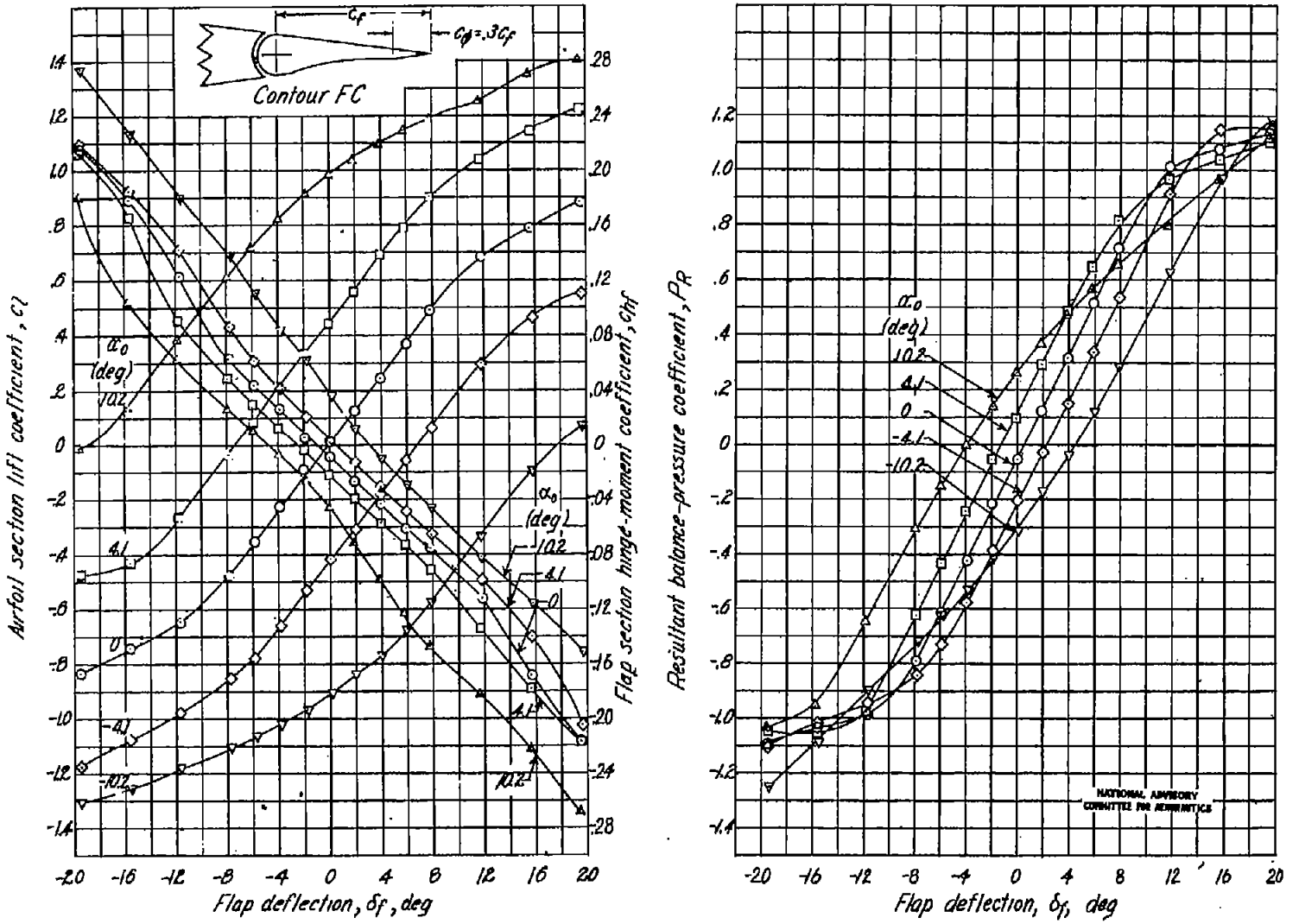

(c) $\frac{c_\phi}{c_f} = 0.3$.

Figure 7.- Concluded.

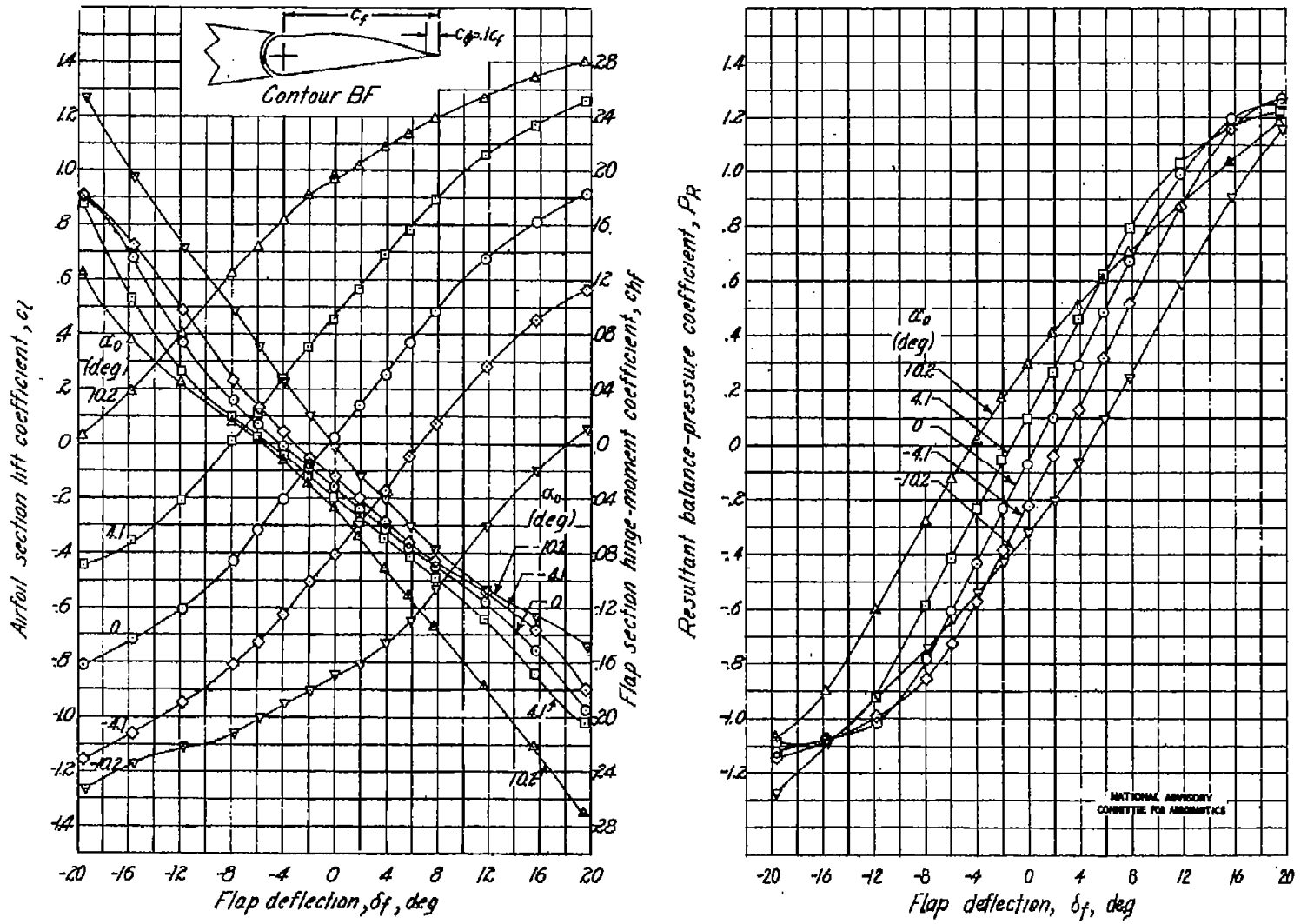

(a) $\frac{c_\phi}{c_f} = 0.1$.

Figure 8.- Section aerodynamic characteristics of modified NACA 65_1-012 airfoil with 0.30c flap. Flap contour BF; gap sealed; transition strips at 0.02c; M, 0.34.

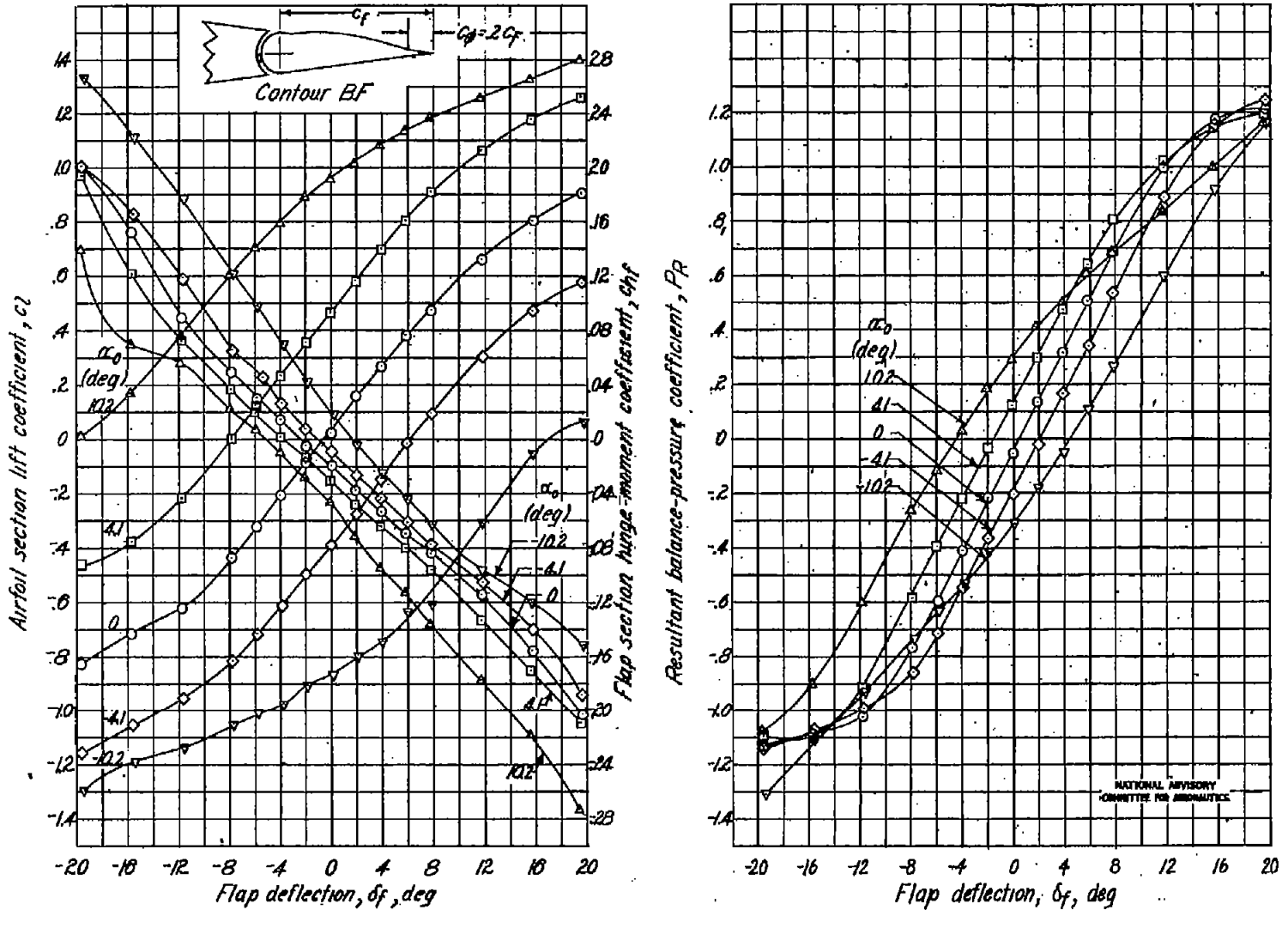

(b) $\frac{c_\phi}{c_f} = 0.2$.

Figure 8.- Continued.

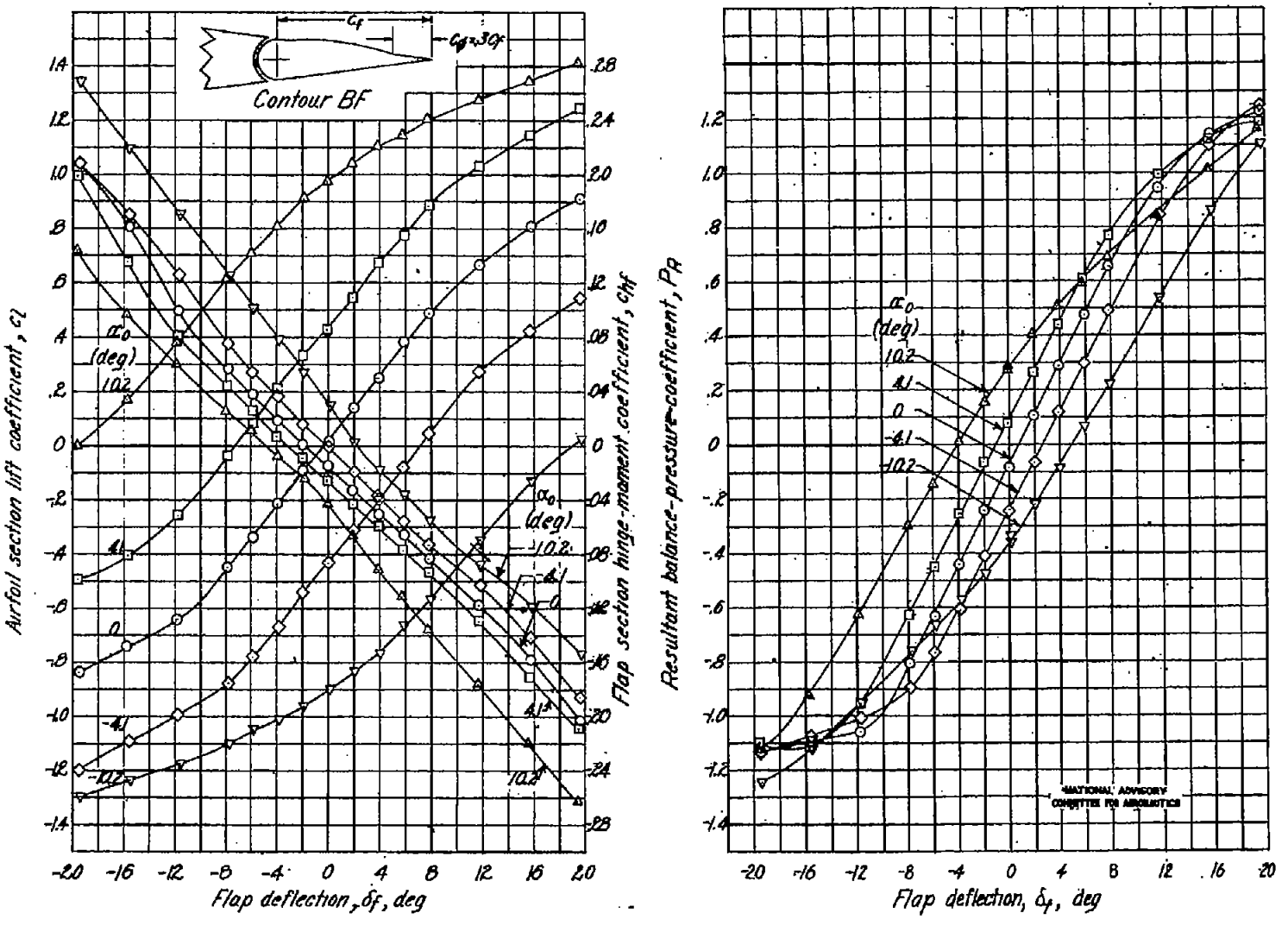

(c) $\frac{c_\phi}{c_f} = 0.3$.

Figure 8.- Concluded.

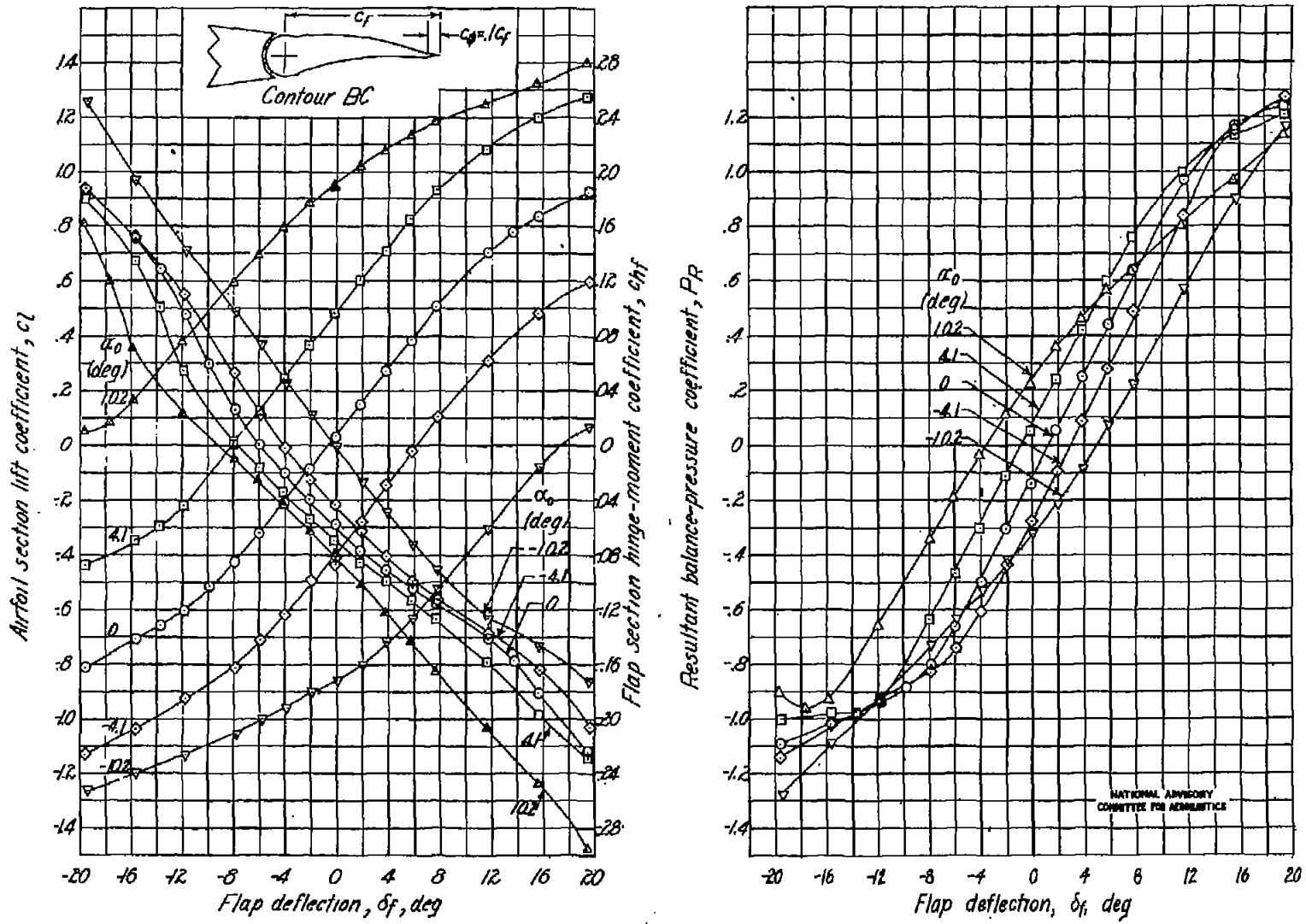

(a) $\frac{c_\phi}{c_f} = 0.1$.

Figure 9.- Section aerodynamic characteristics of modified NACA 65_1-012 airfoil with 0.30c flap.

Flap contour BC: gap sealed; transition strips at 0.02c; M, 0.24

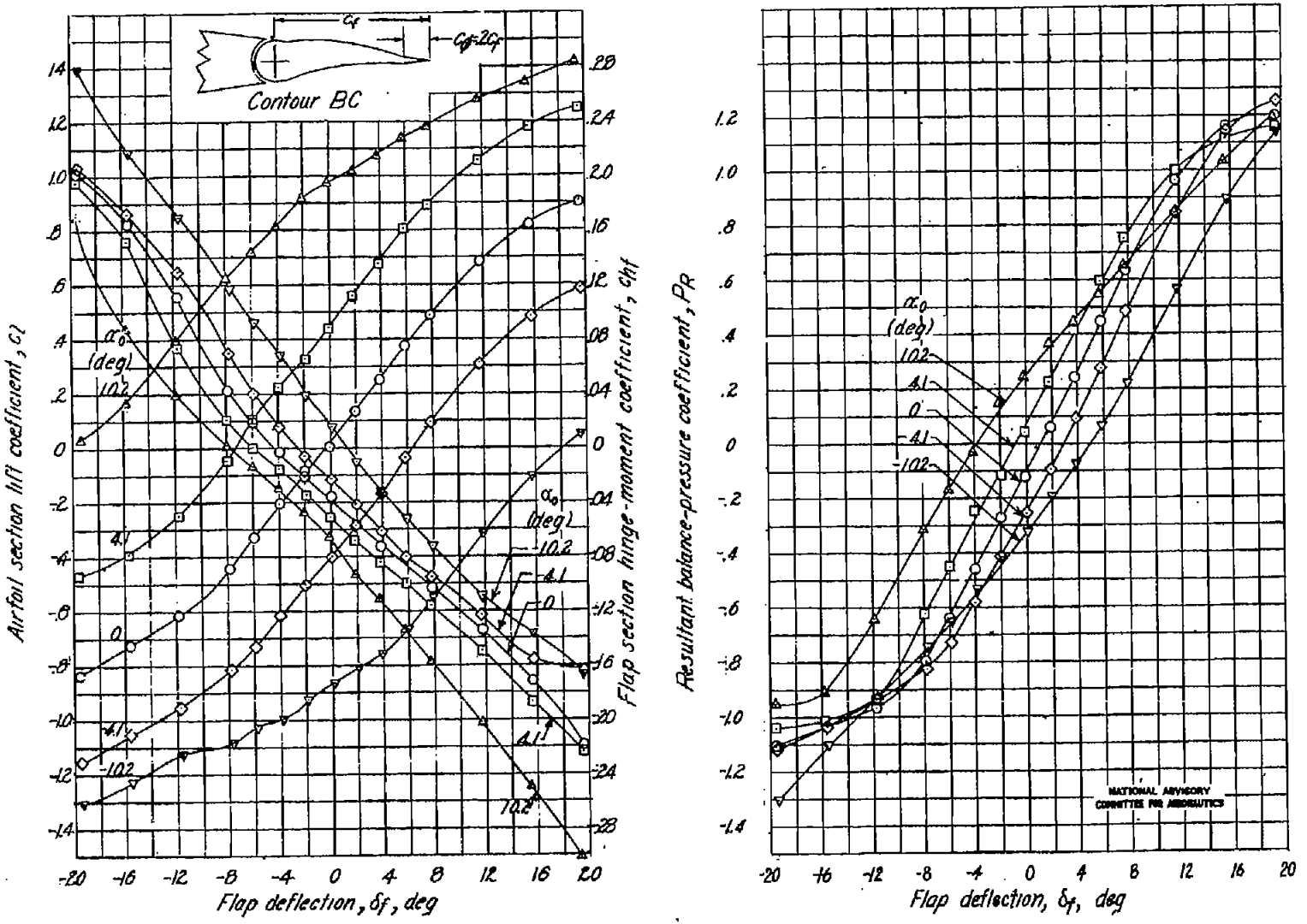

(b) $\frac{c_\phi}{c_f} = 0.2$.

Figure 9.- Continued.

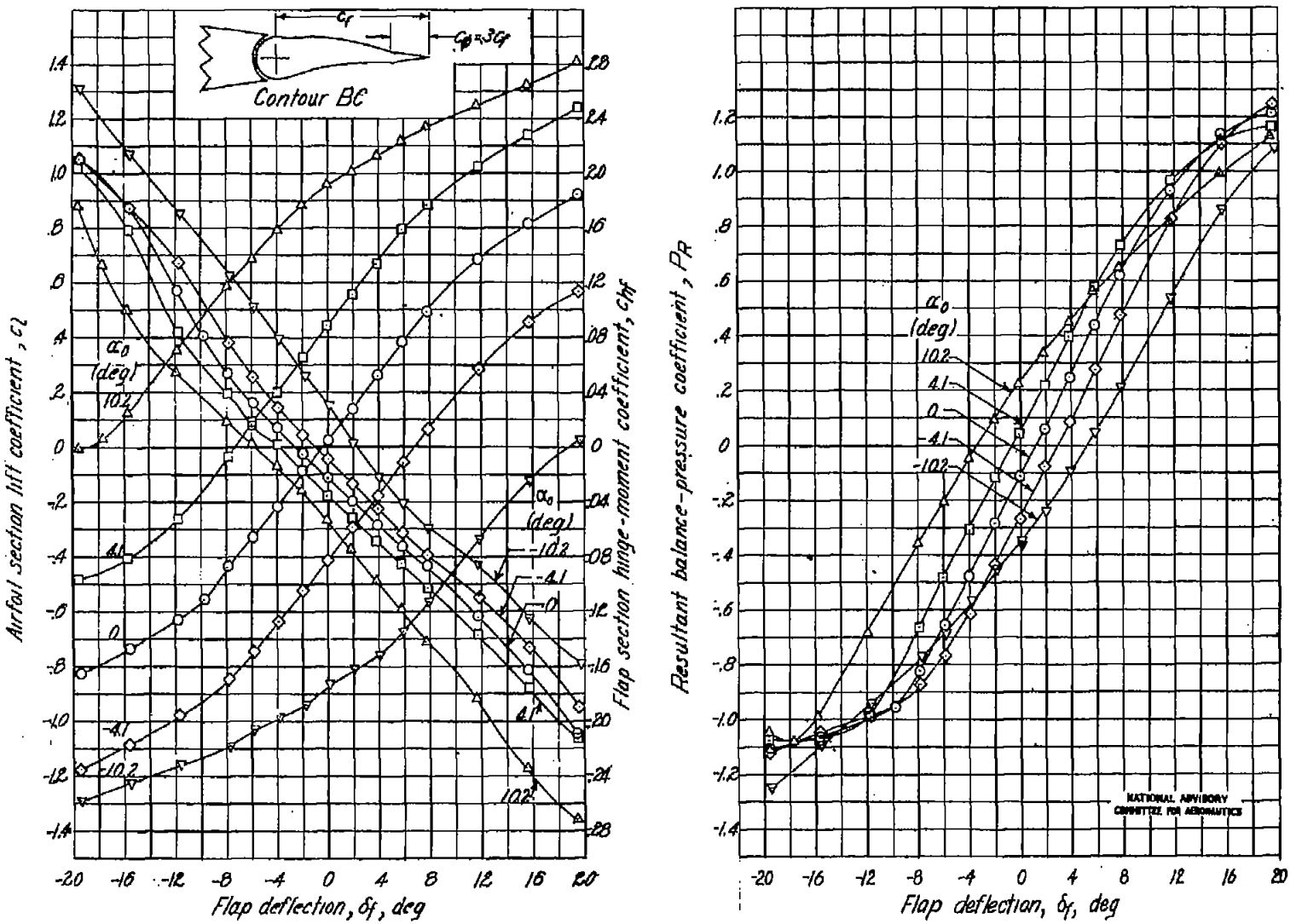

(c) $\frac{c_\phi}{c_f} = 0.3$.

Figure 9.- Concluded.

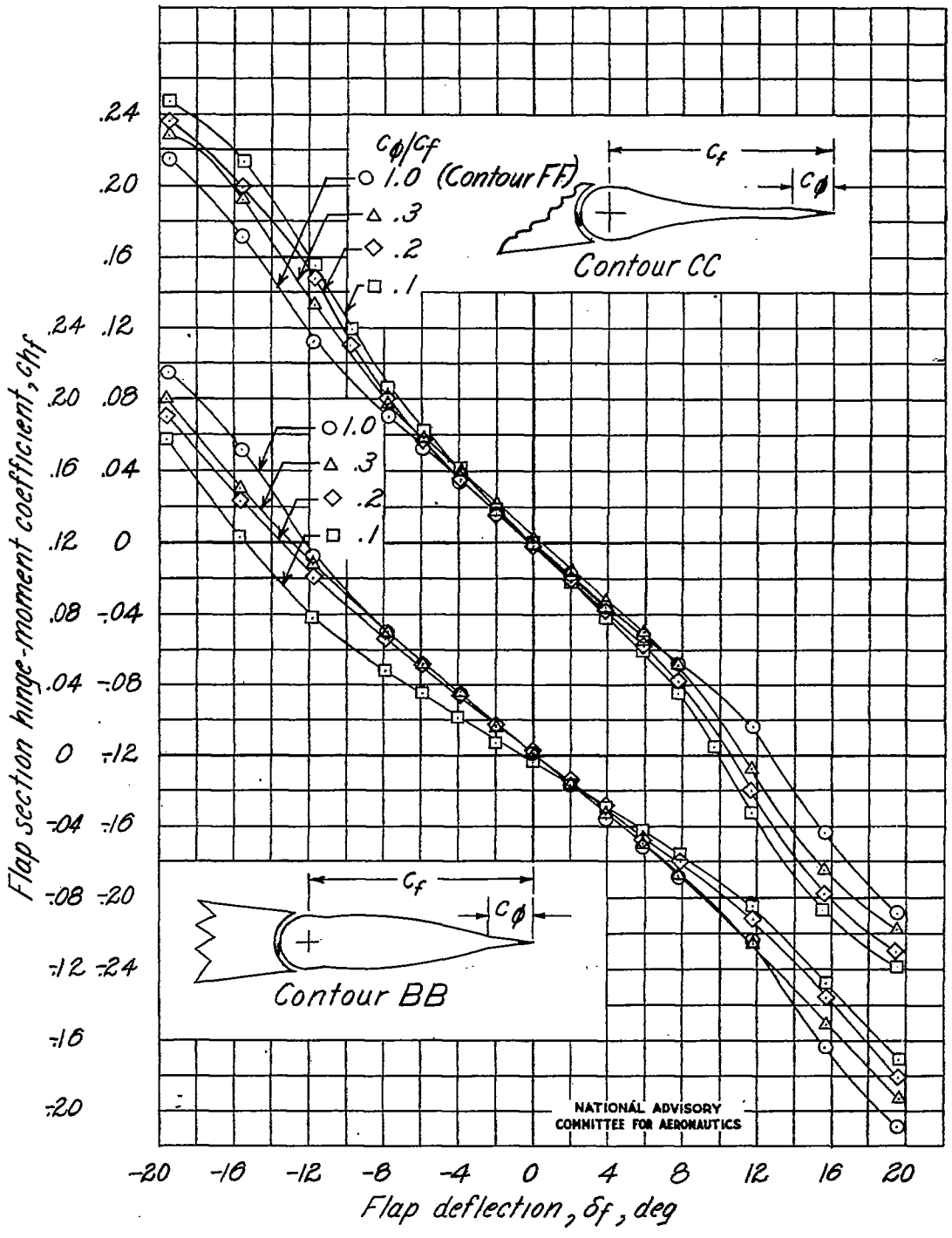

Figure 10.- Effect of fixed trailing-edge chord on the variation of flap section hinge-moment coefficient with flap deflection. Modified NACA 65_1-012 airfoil; transition strips at 0.02c; gap sealed; M, 0.34; $\alpha_o = 0°$.

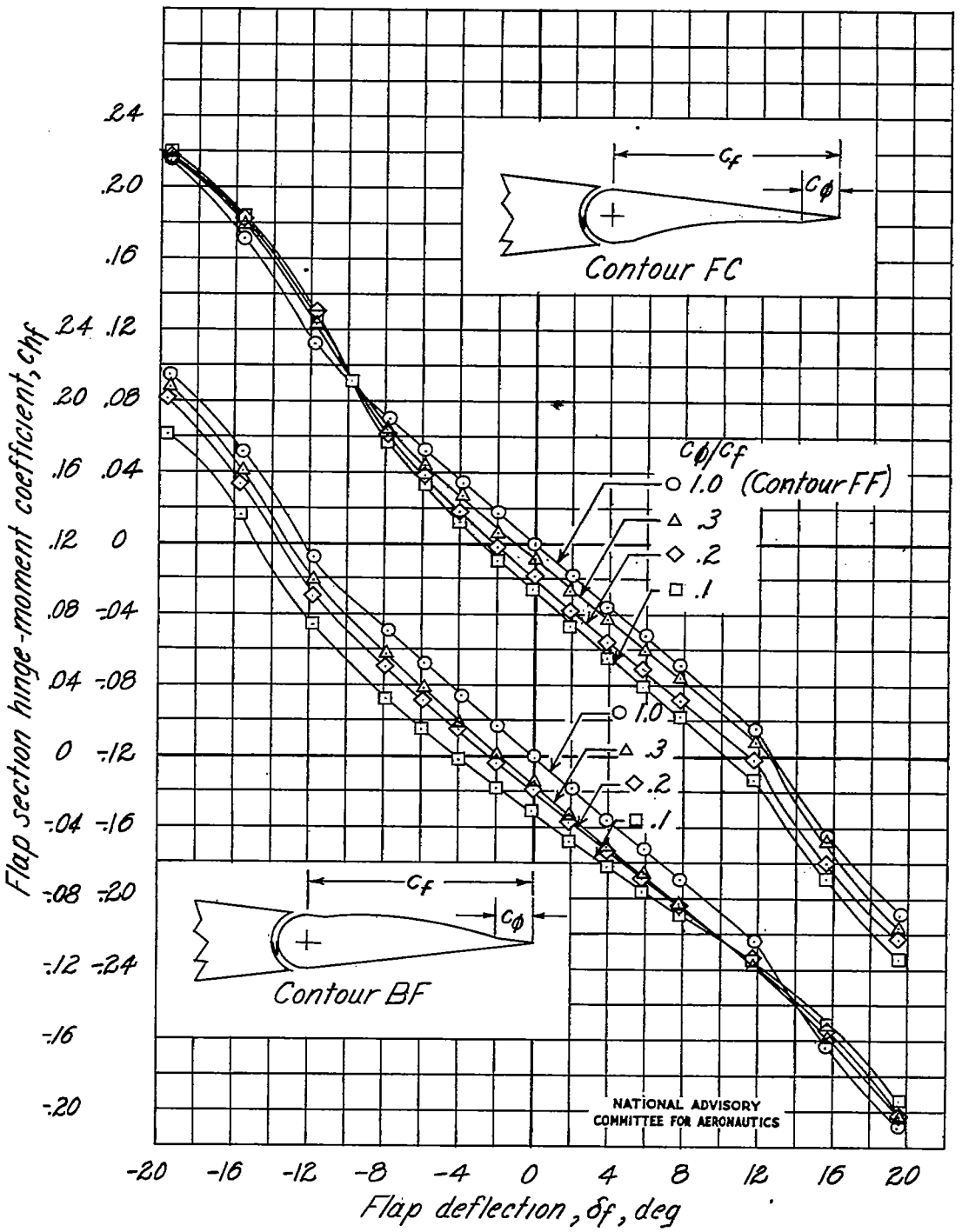

Figure 10.- Continued.

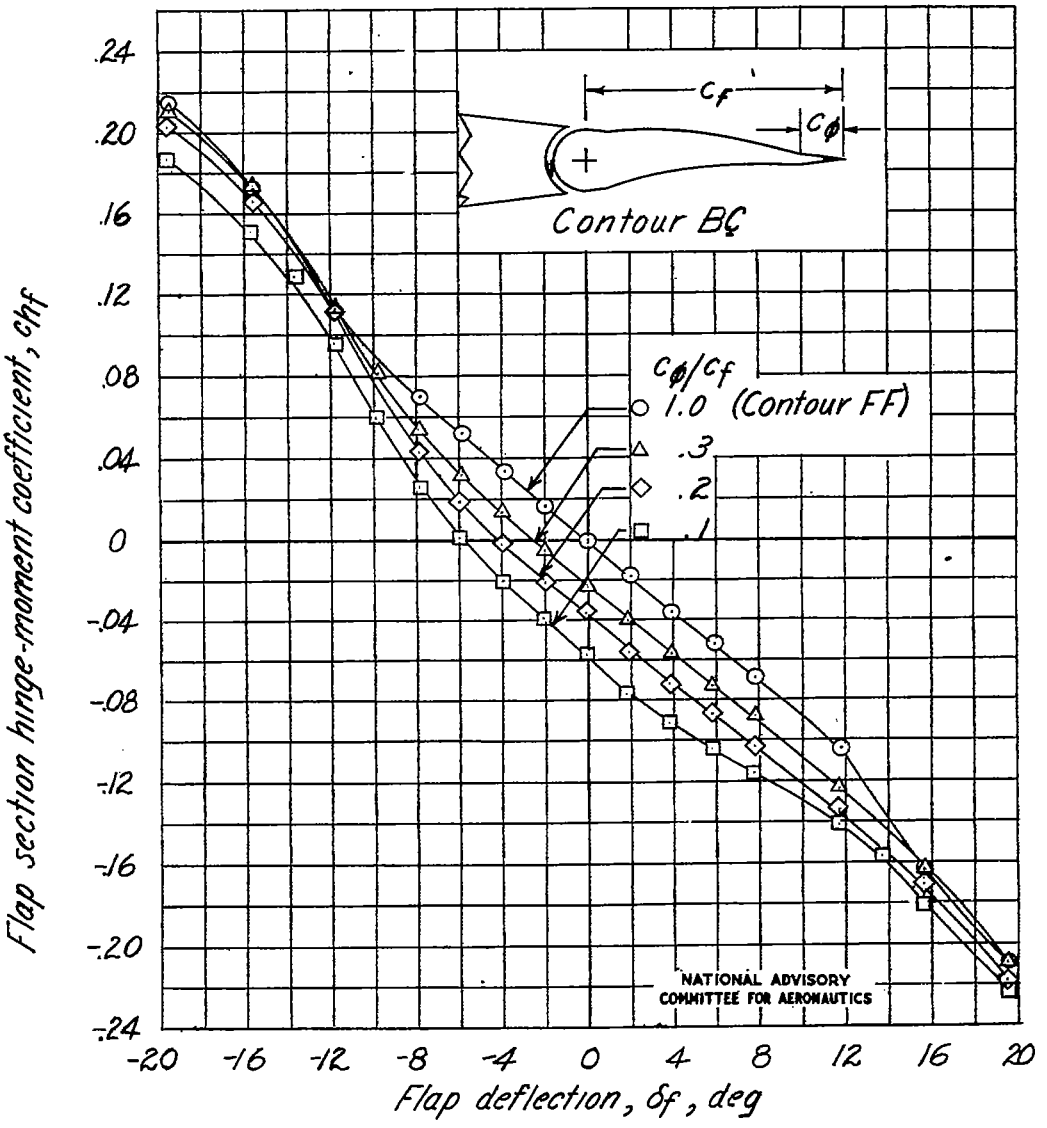

Figure 10.- Concluded.

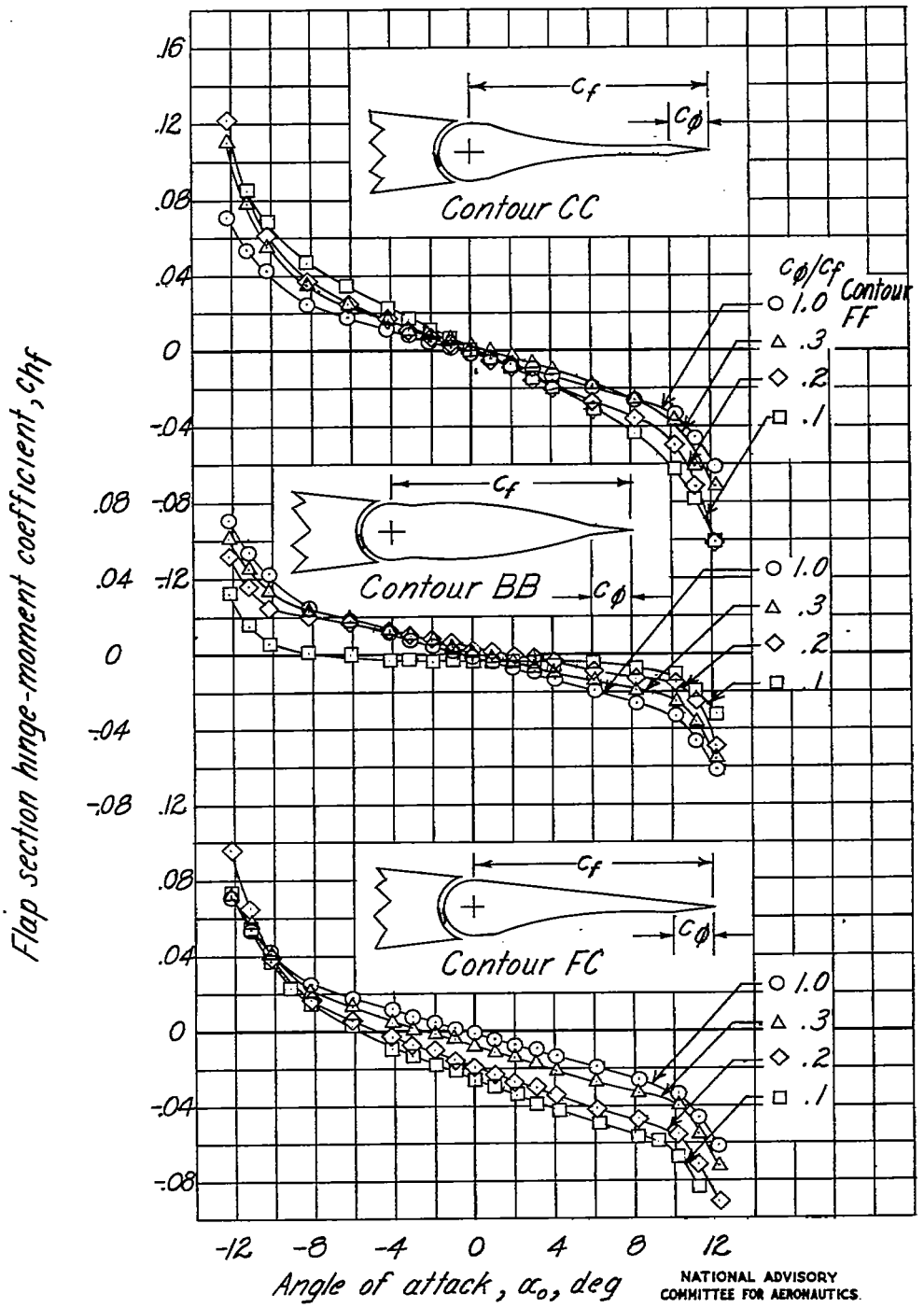

Figure 11.- Effect of fixed trailing-edge chord on the variation of flap section hinge-moment coefficient with angle of attack. Modified NACA 65_1-012 airfoil; transition strips at 0.02c; gap sealed; M, 0.34; $\delta_f = 0^\circ$.

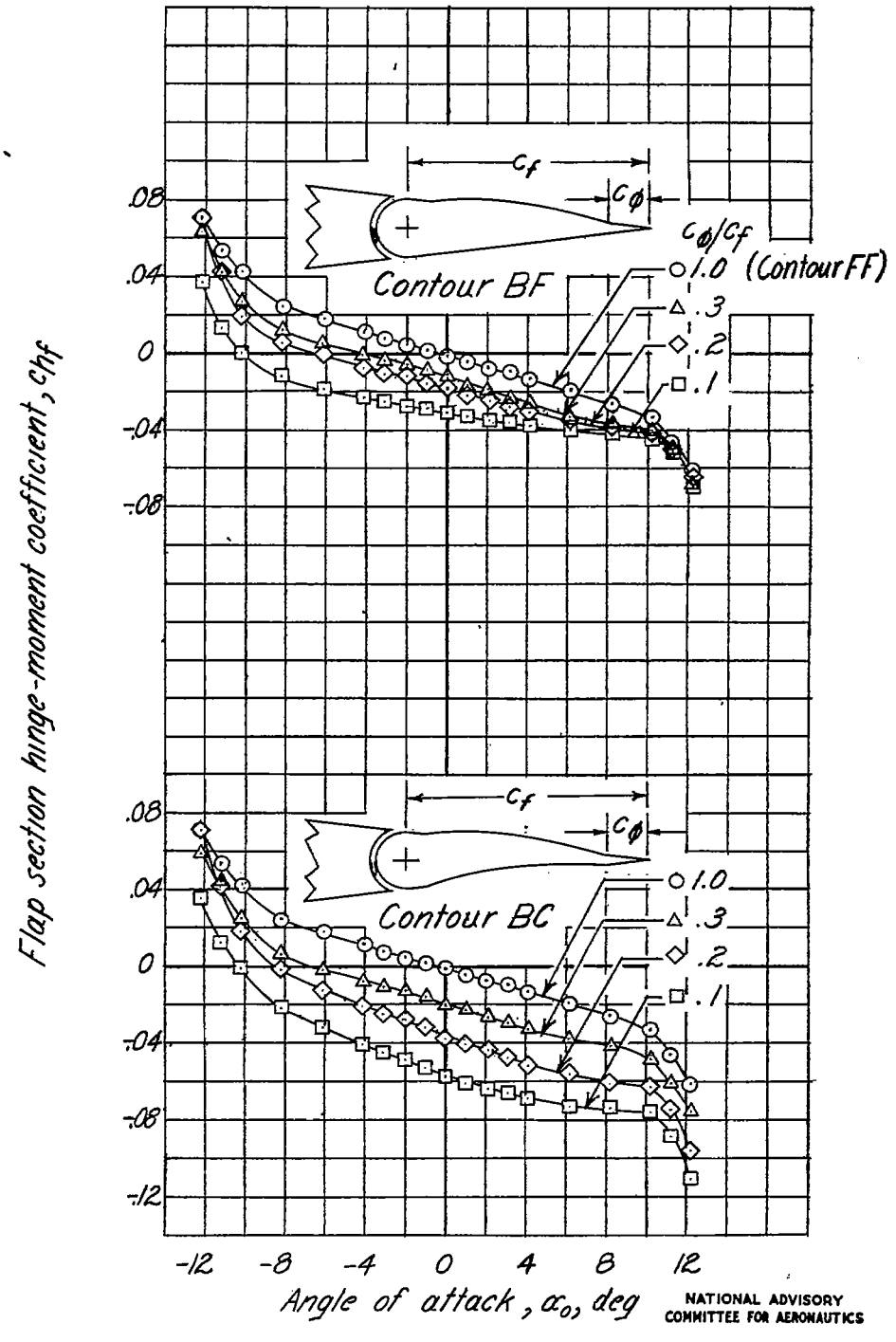

Figure 11.- Concluded.

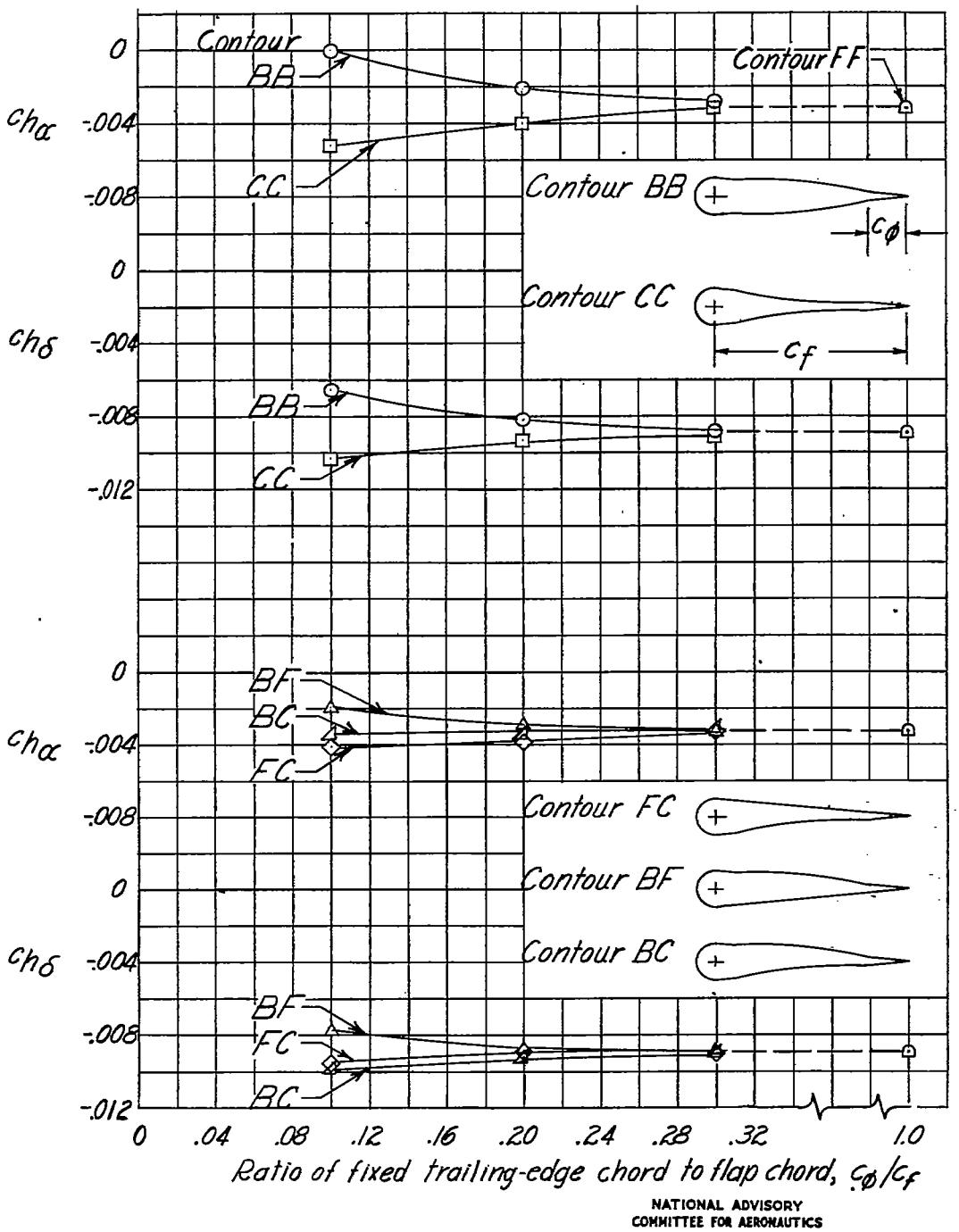

Figure 12.- Effect of fixed trailing-edge chord on the hinge-moment slopes of flaps having distorted contours. Slopes measured at $\alpha_o = 0^\circ$, $\delta_f = 0^\circ$; transition strips at 0.02c; gap sealed; M, 0.34.

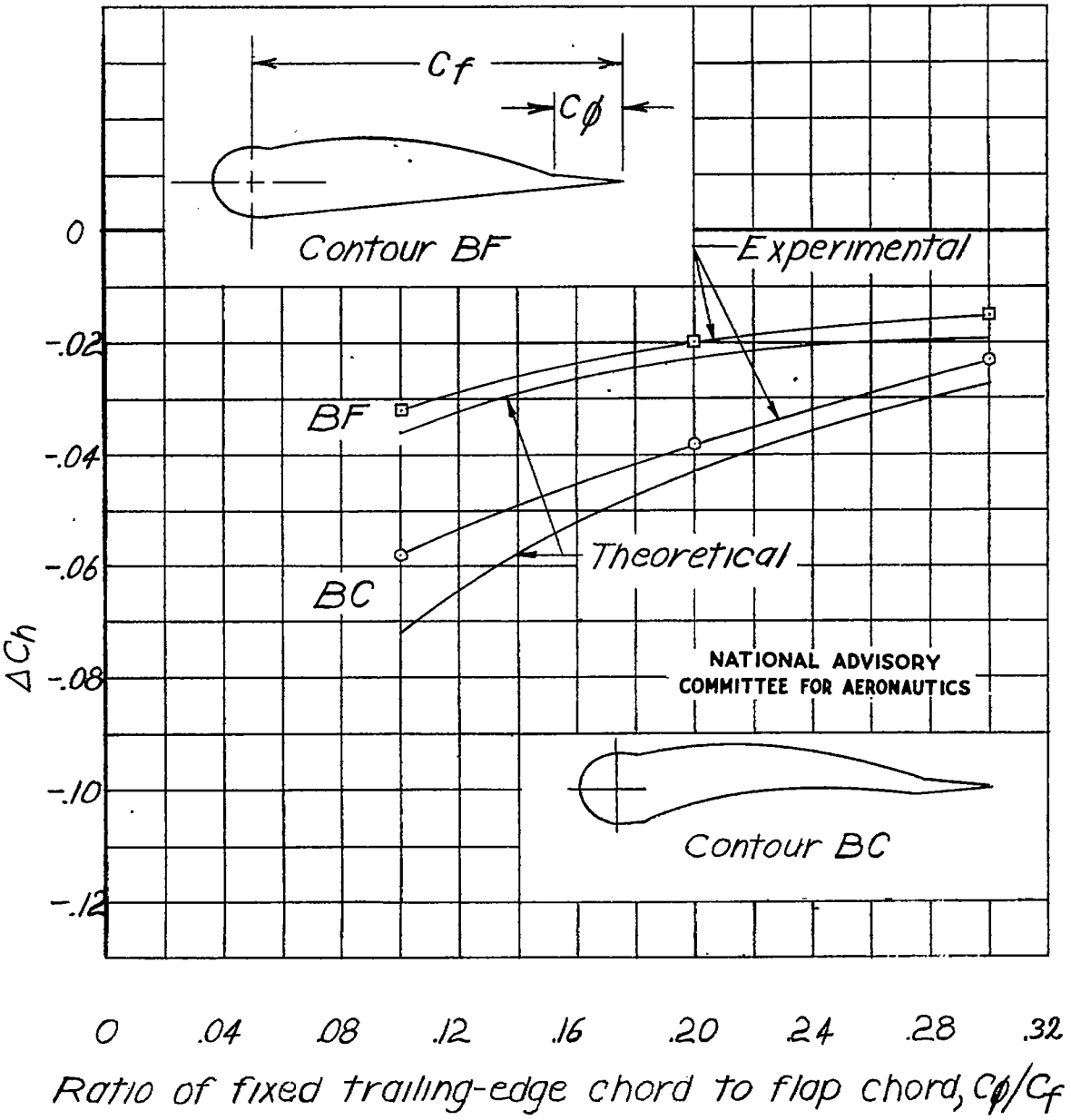

Figure 13.- Effect of fixed trailing-edge chord on the hinge-moment increment resulting from distortion. Increments measured at $\alpha_o = 0^\circ$, $\delta_f = 0^\circ$; transition strips at 0.02c; gap sealed; M, 0.34.

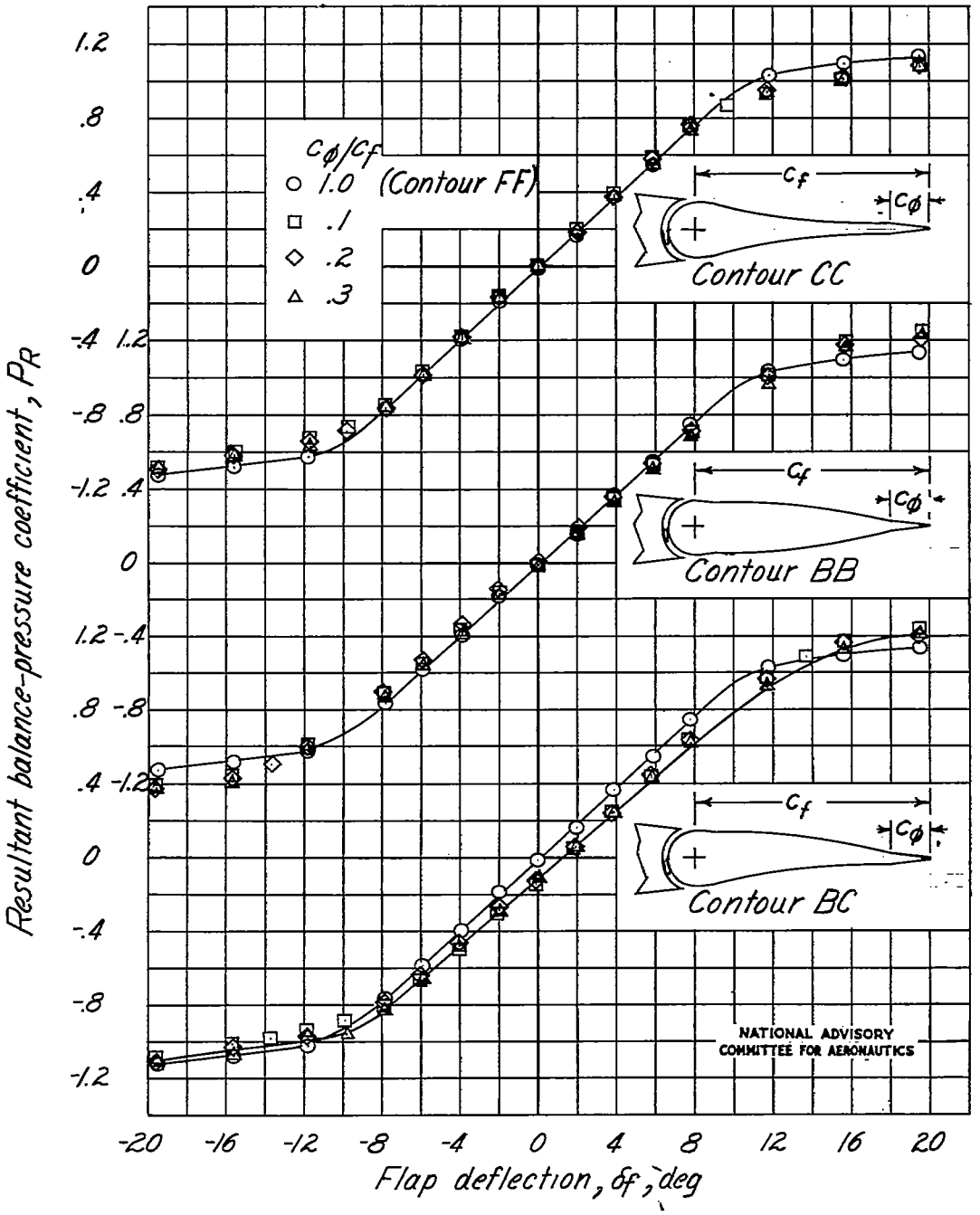

Figure 14.- Effect of fixed trailing-edge chord on the variation of resultant balance-pressure coefficient with flap deflection. Modified NACA 65_1-012 airfoil; transition strips at 0.02c; gap sealed; M, 0.34; $\alpha_o = 0^\circ$.

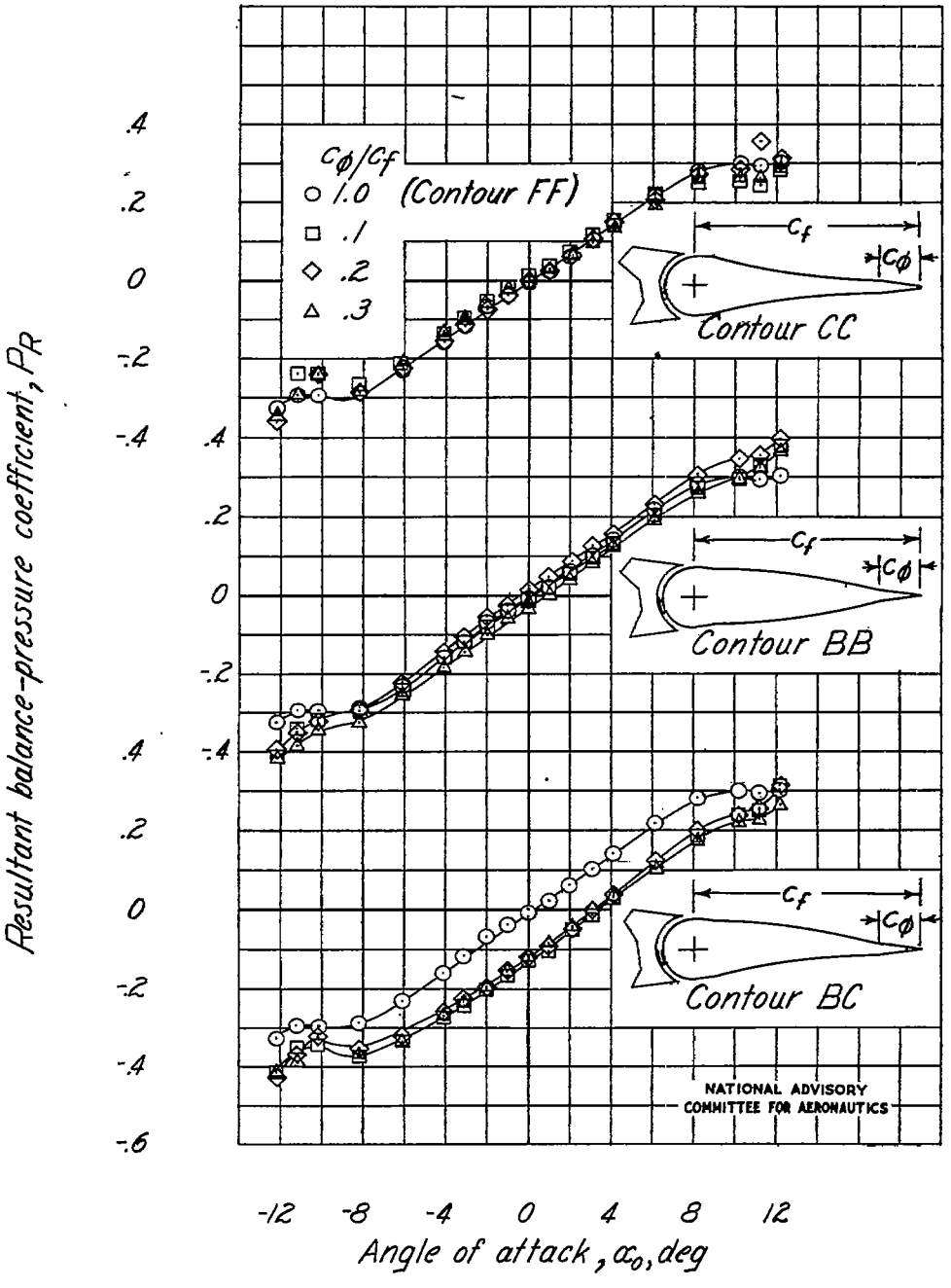

Figure 15.- Effect of fixed trailing-edge chord on the variation of resultant balance-pressure coefficient with angle of attack. Modified NACA 65_1-012 airfoil; transition strips at 0.02c; gap sealed; M, 0.34; $\delta_f = 0^\circ$.

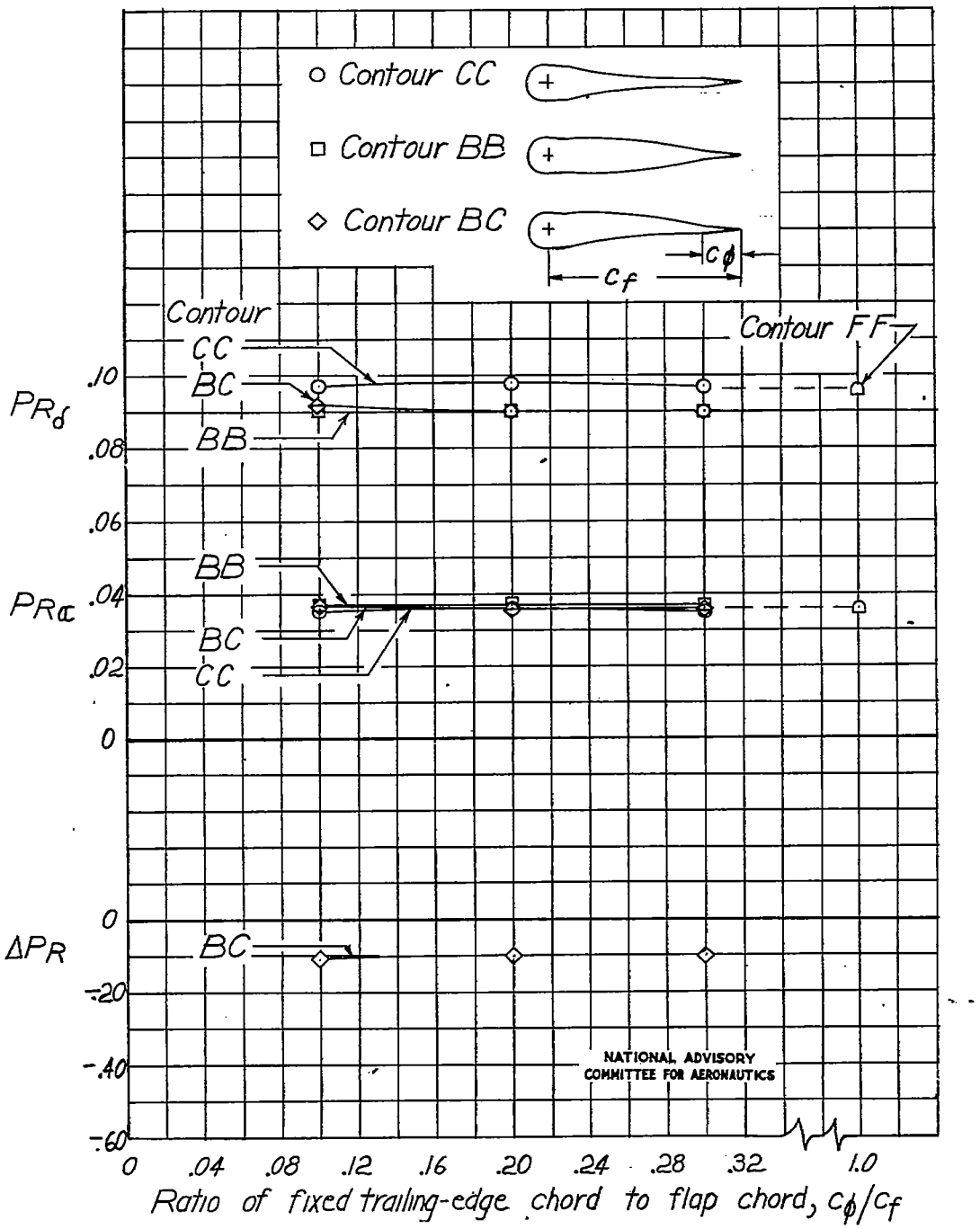

Figure 16.- Effect of fixed trailing-edge chord on the resultant balance-pressure parameters of flaps having distorted contours. Parameters measured at $\alpha_o = 0^\circ$; $\delta_f = 0^\circ$; transition strips at 0.02c; gap sealed; M, 0.34.

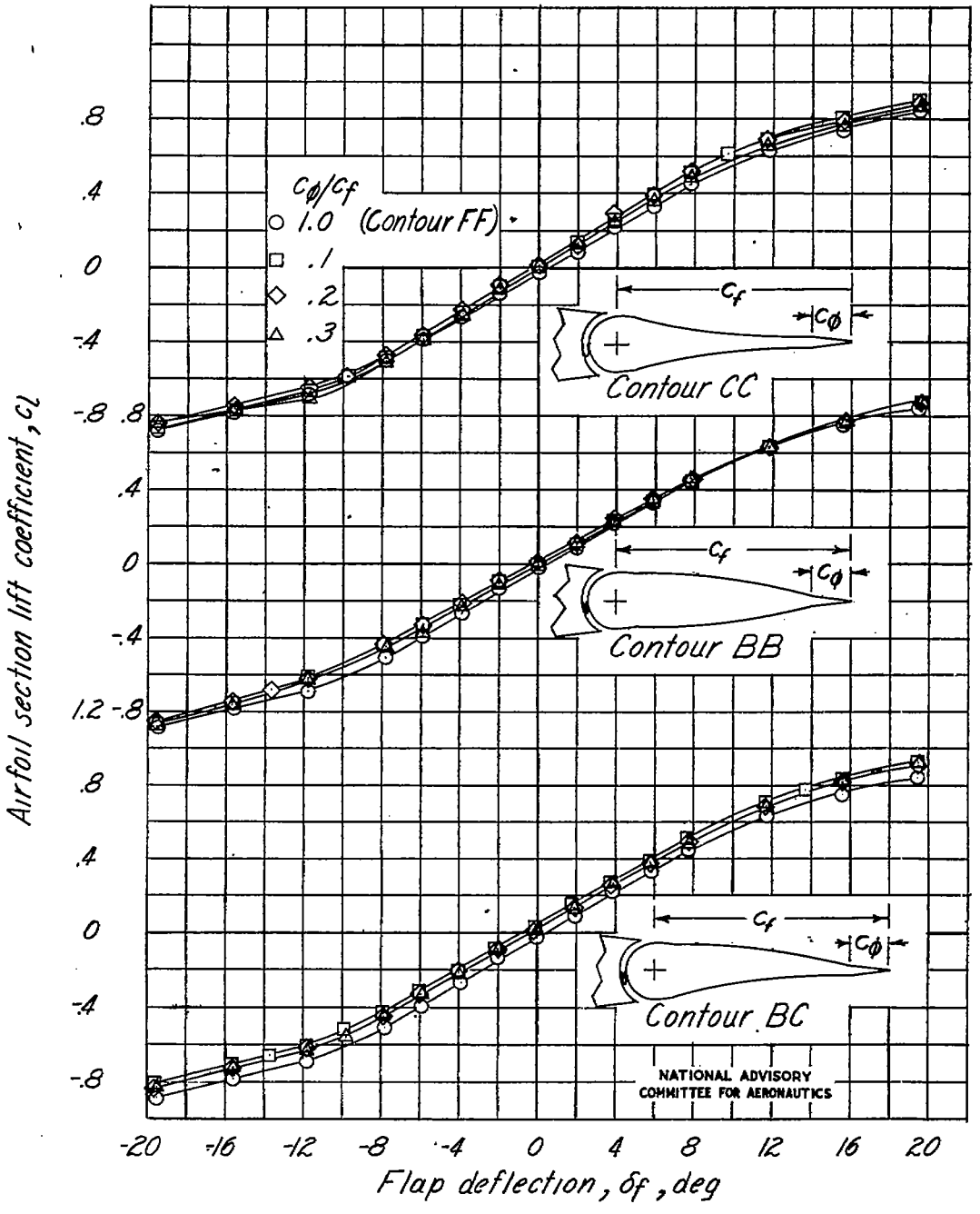

Figure 17.- Effect of fixed trailing-edge chord on the variation of airfoil section lift coefficient with flap deflection. Modified NACA 65_1-012 airfoil; transition strips at 0.02c; gap sealed; M, 0.34; $\alpha_o = 0^\circ$.

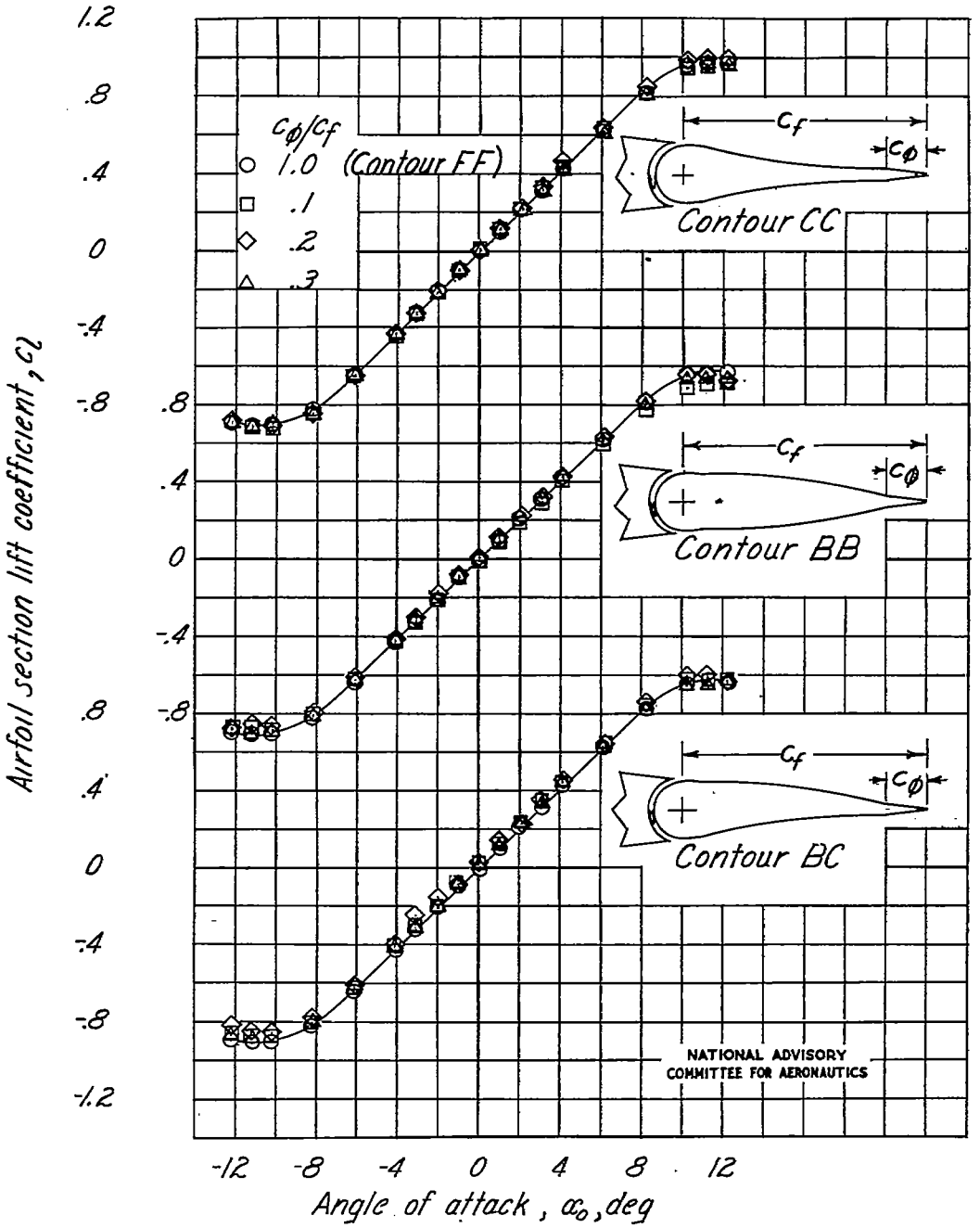

Figure 18.- Effect of fixed trailing-edge chord on the variation of airfoil section lift coefficient with angle of attack. Modified NACA 65_1-012 airfoil; transition strips at 0.02c; gap sealed; M, 0.34; $\delta_f = 0^\circ$.

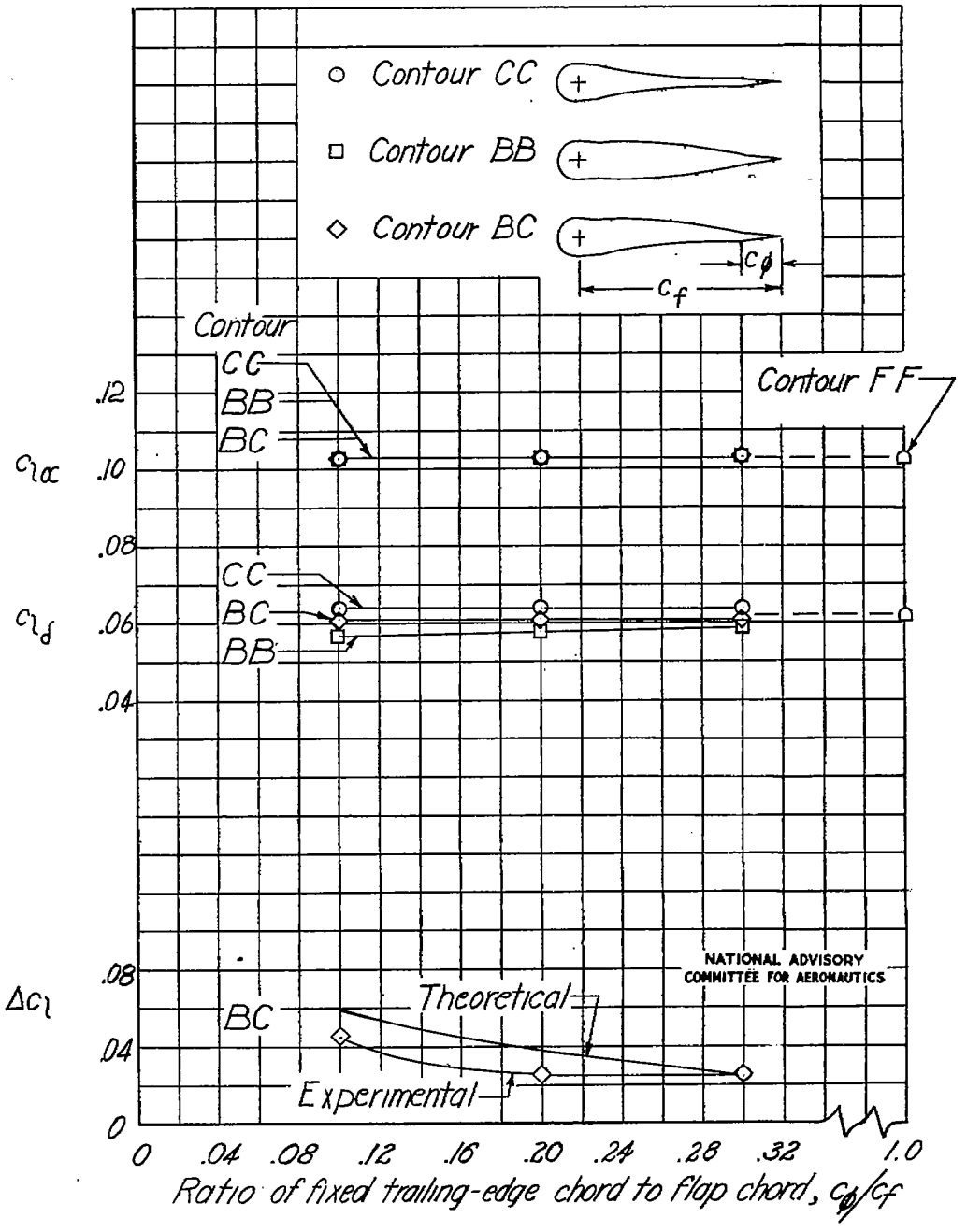

Figure 19.- Effect of fixed trailing-edge chord on the lift parameters of flaps having distorted contours. Parameters measured at $\alpha_o = 0^\circ$, $\delta_f = 0^\circ$; transition strips at 0.02c; gap sealed; M, 0.34.

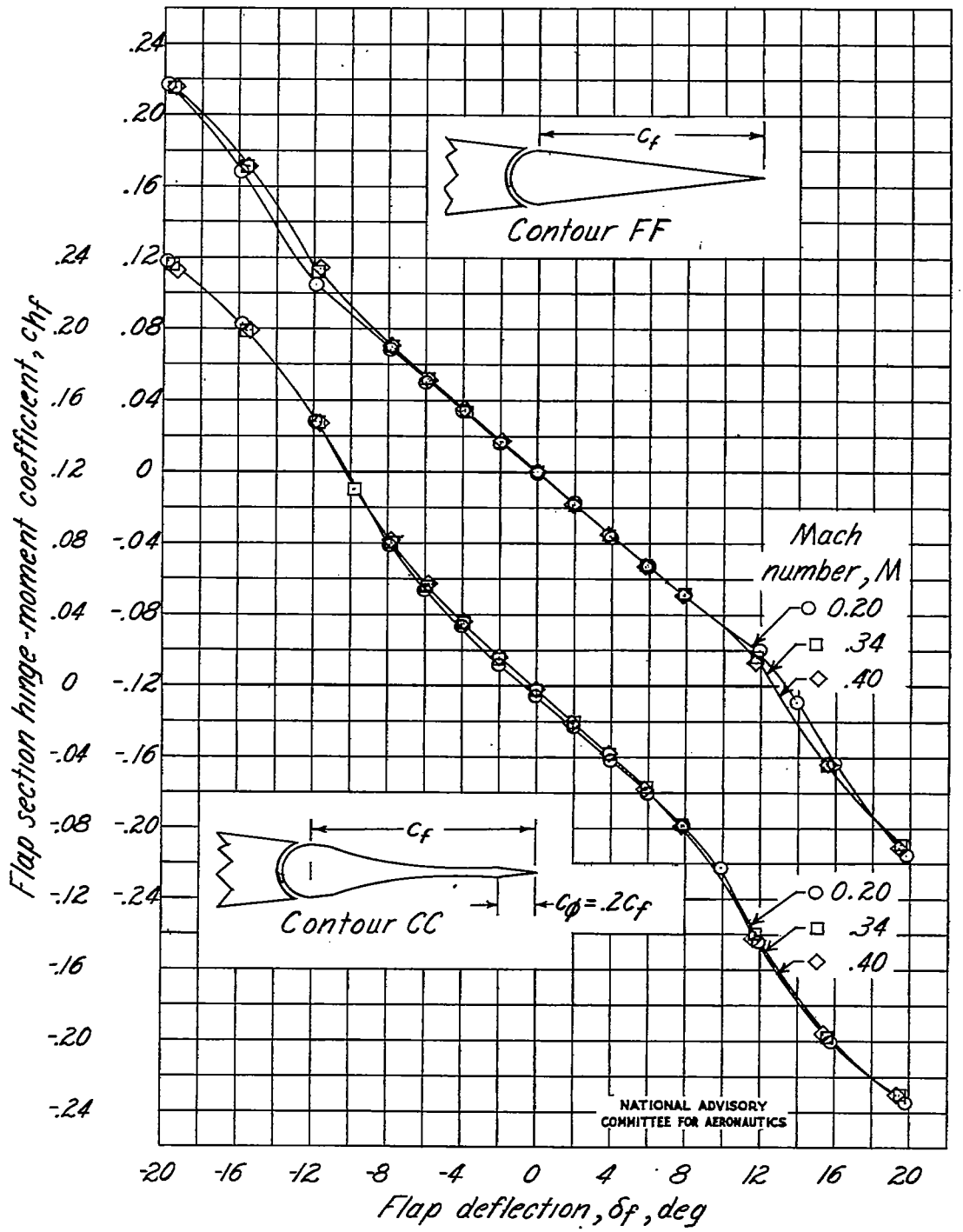

Figure 20.- Effect of Mach number on the variation of flap section hinge-moment coefficient with flap deflection. Modified NACA 65_1-012 airfoil; $\frac{c_\phi}{c_f} = 0.20$ (except for contour FF); transition strips at 0.02c; gap sealed; $\alpha_o = 0^\circ$.

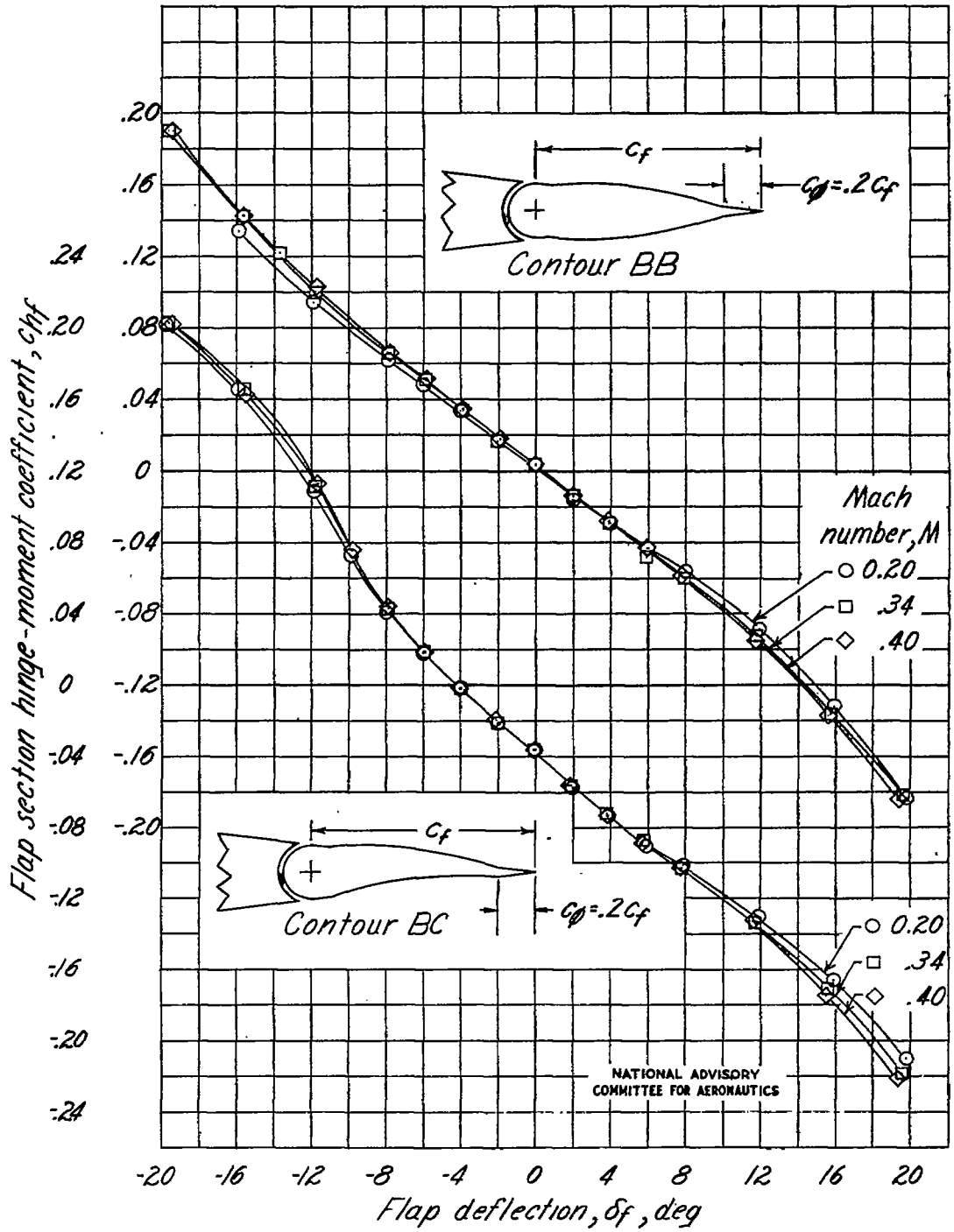

Figure 20.- Concluded.

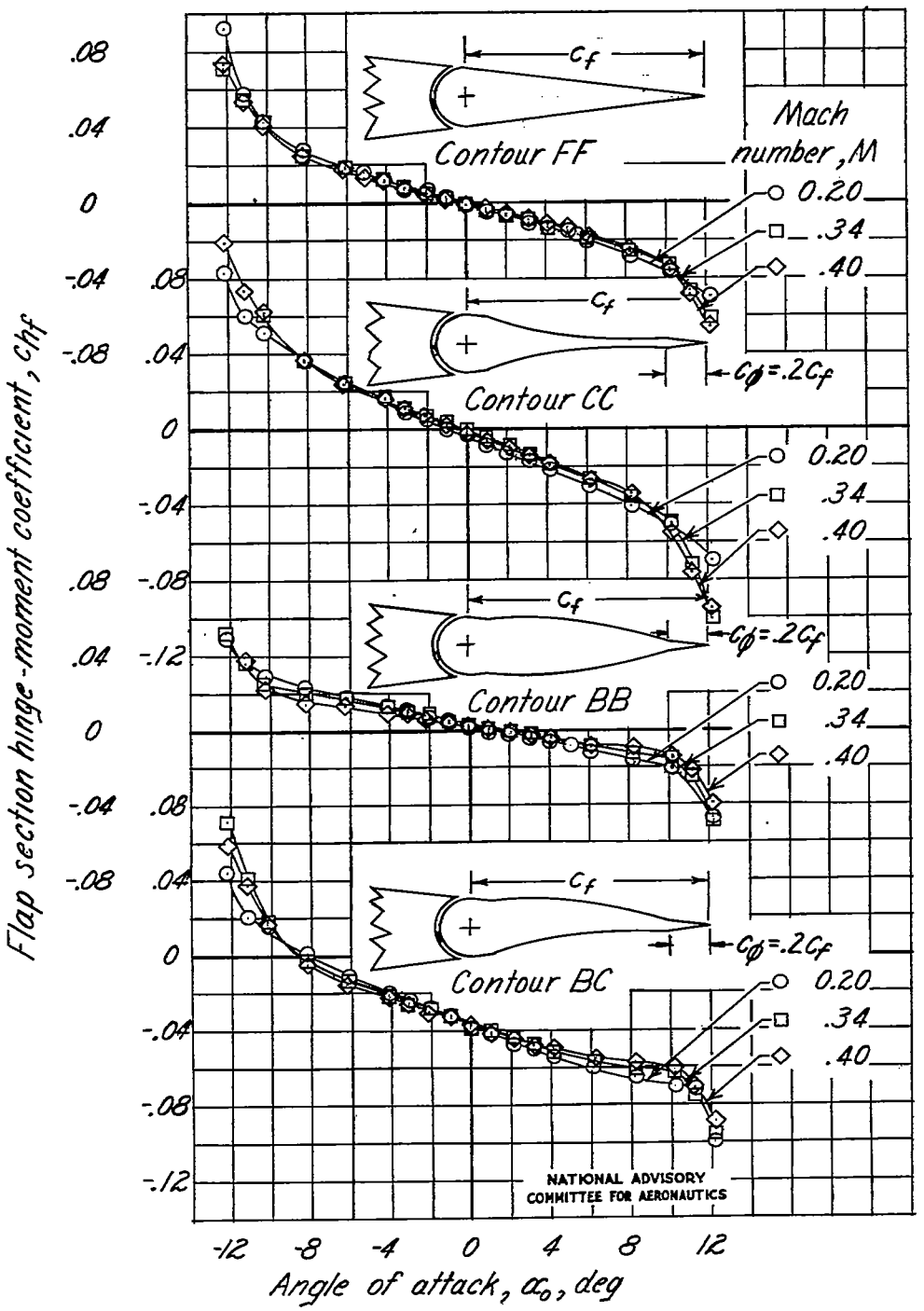

Figure 21.- Effect of Mach number on the variation of flap section hinge-moment coefficient with angle of attack. Modified NACA 65_1-012 airfoil; $\frac{c_\phi}{c_f} = 0.2$ (except for contour FF); transition strips at 0.02c; gap sealed; $\delta_f = 0^\circ$.

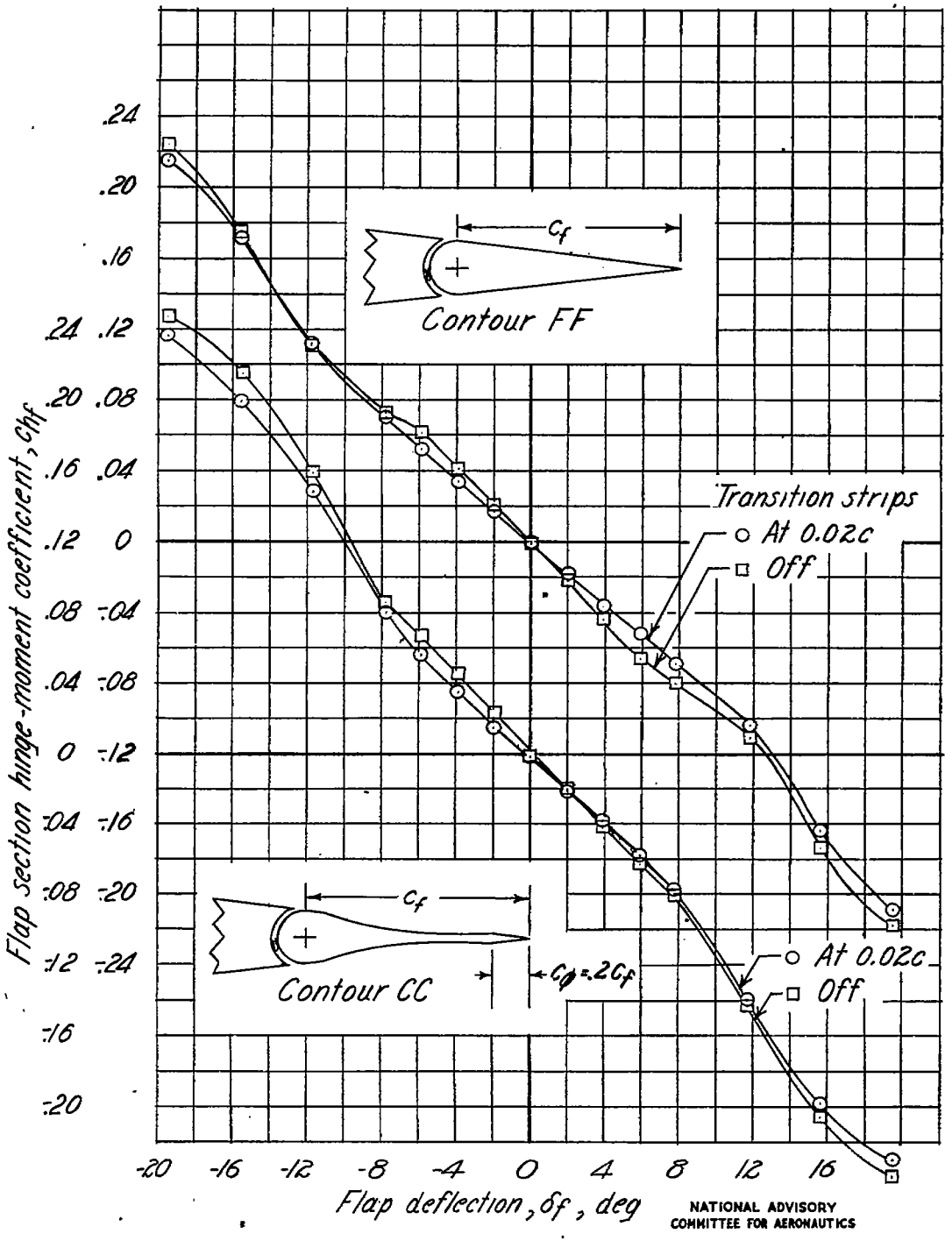

Figure 22.- Effect of transition strips on the variation of flap section hinge-moment coefficient with flap deflection. Modified NACA 65_1-012 airfoil; $\frac{c_\phi}{c_f} = 0.2$ (except for contour FF); gap sealed; M, 0.34; $\alpha_o = 0^\circ$.

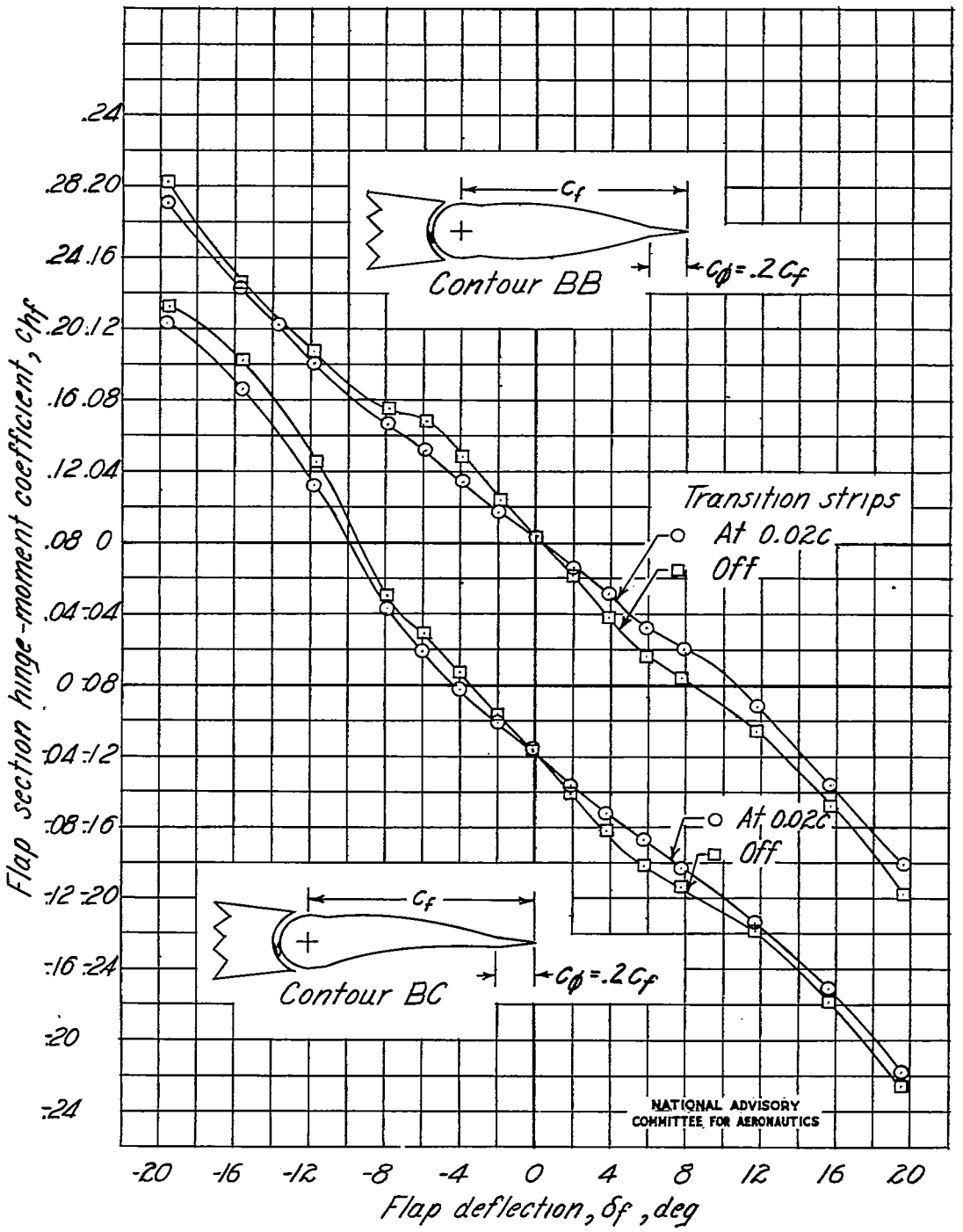

Figure 22.- Concluded.

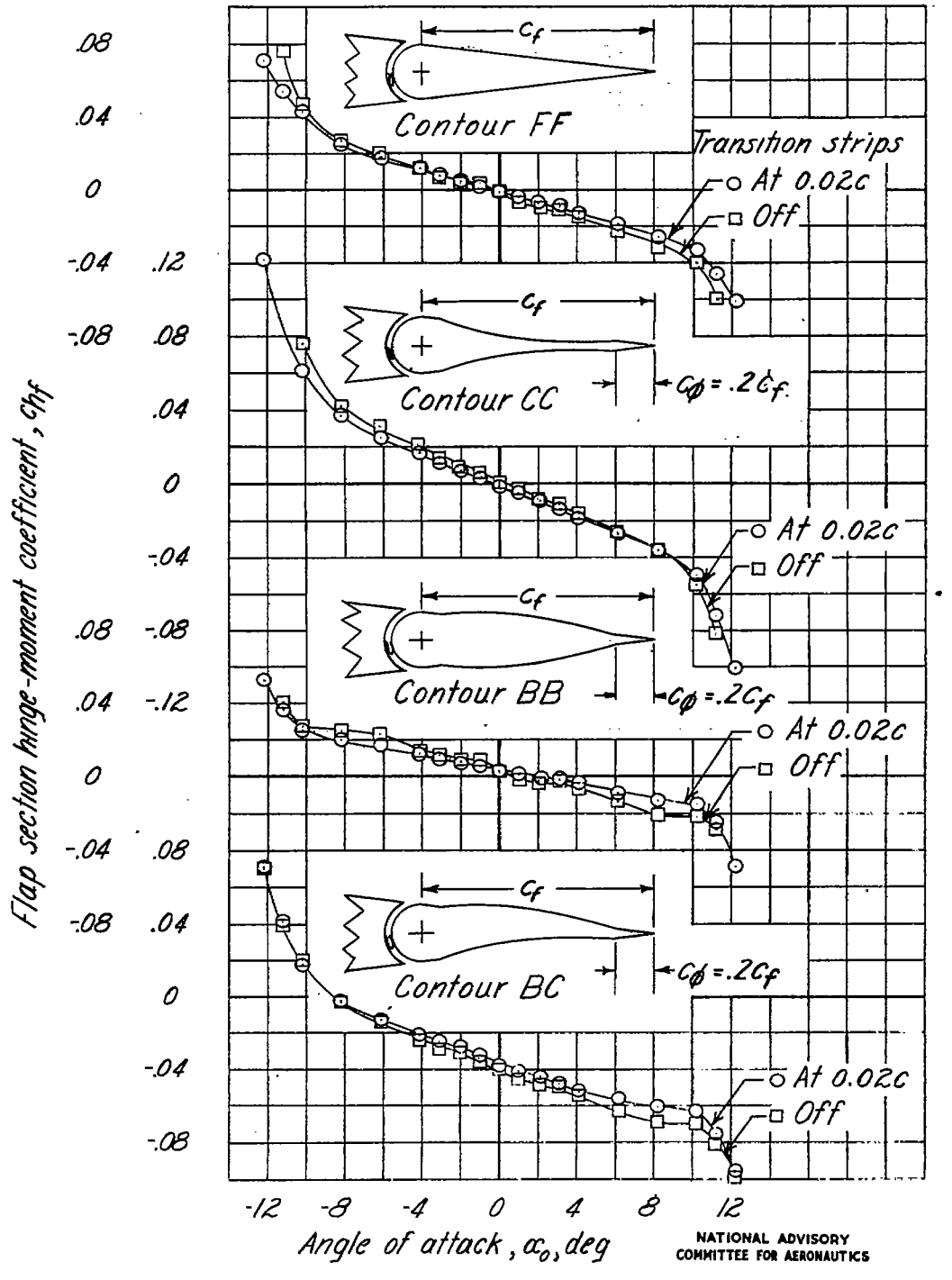

Figure 23.- Effect of transition strips on the variation of flap section hinge-moment coefficient with angle of attack. Modified NACA 65_1-012 airfoil; $\frac{c_\phi}{c_f} = 0.2$ (except for contour FF); gap sealed; M, 0.34; $\delta_f = 0^\circ$.

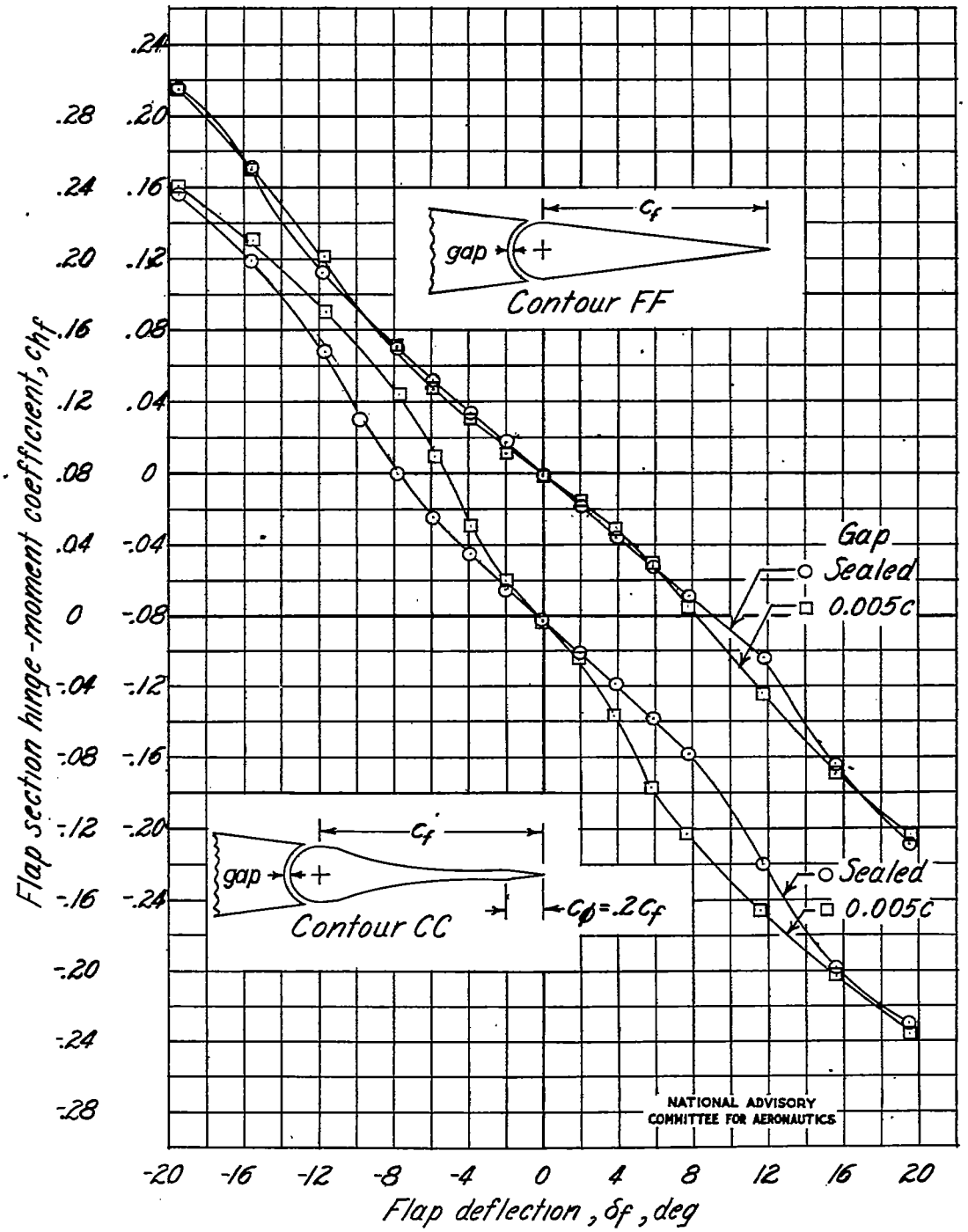

Figure 24.- Effect of gap on the variation of flap section hinge-moment coefficient with flap deflection. Modified NACA 65_1-012 airfoil; $\frac{c_\phi}{c_f} = 0.2$ (except for contour FF); transition strips at 0.02c; M, 0.34; $\alpha_o = 0^\circ$.

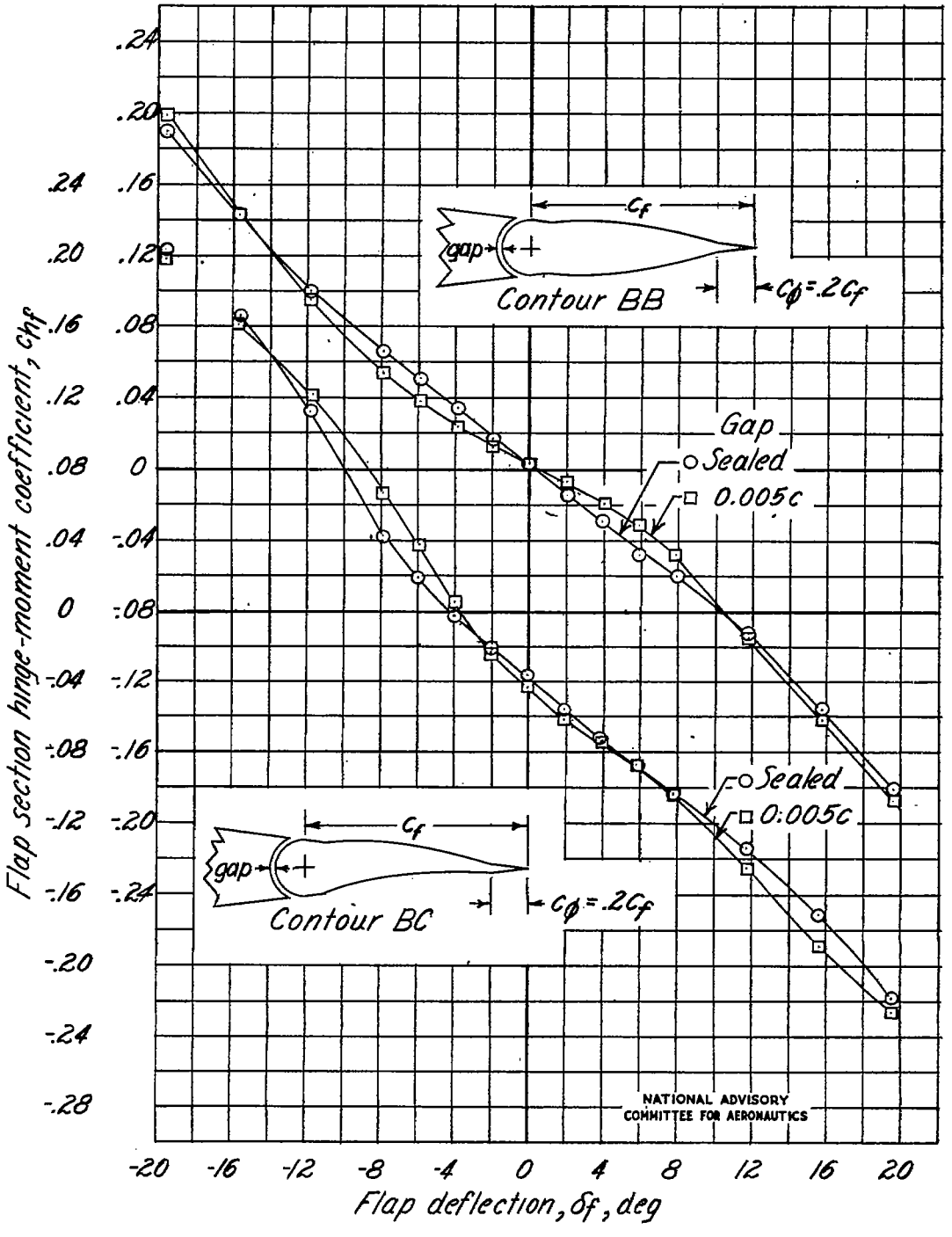

Figure 24.- Concluded.

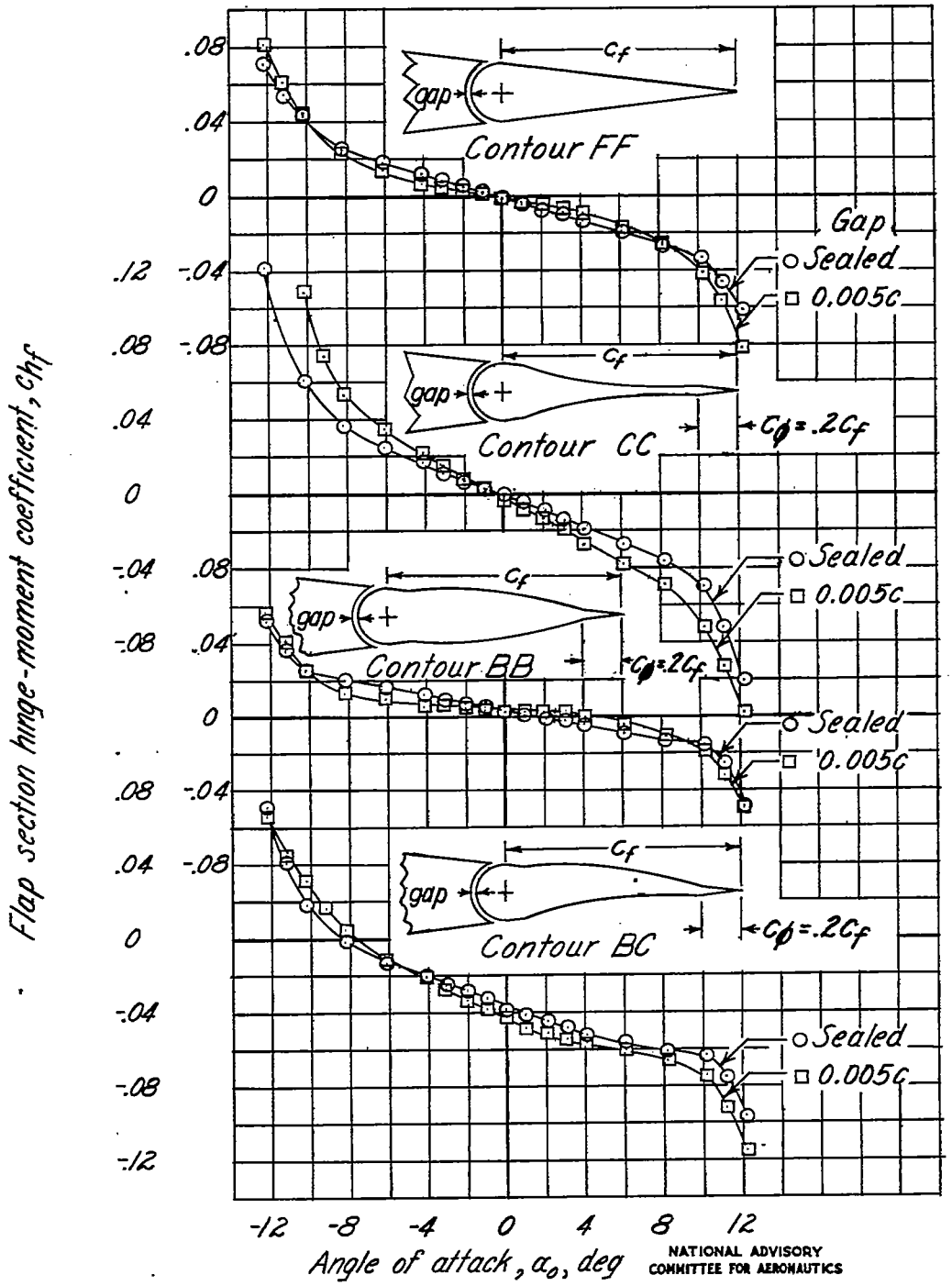

Figure 25.- Effect of gap on the variation of flap section hinge-moment coefficient with angle of attack. Modified NACA 65_1-012 airfoil; $\frac{c_\phi}{c_f} = 0.2$ (except for contour FF); transition strips at 0.02c; M, 0.34; $\delta_f = 0^\circ$.

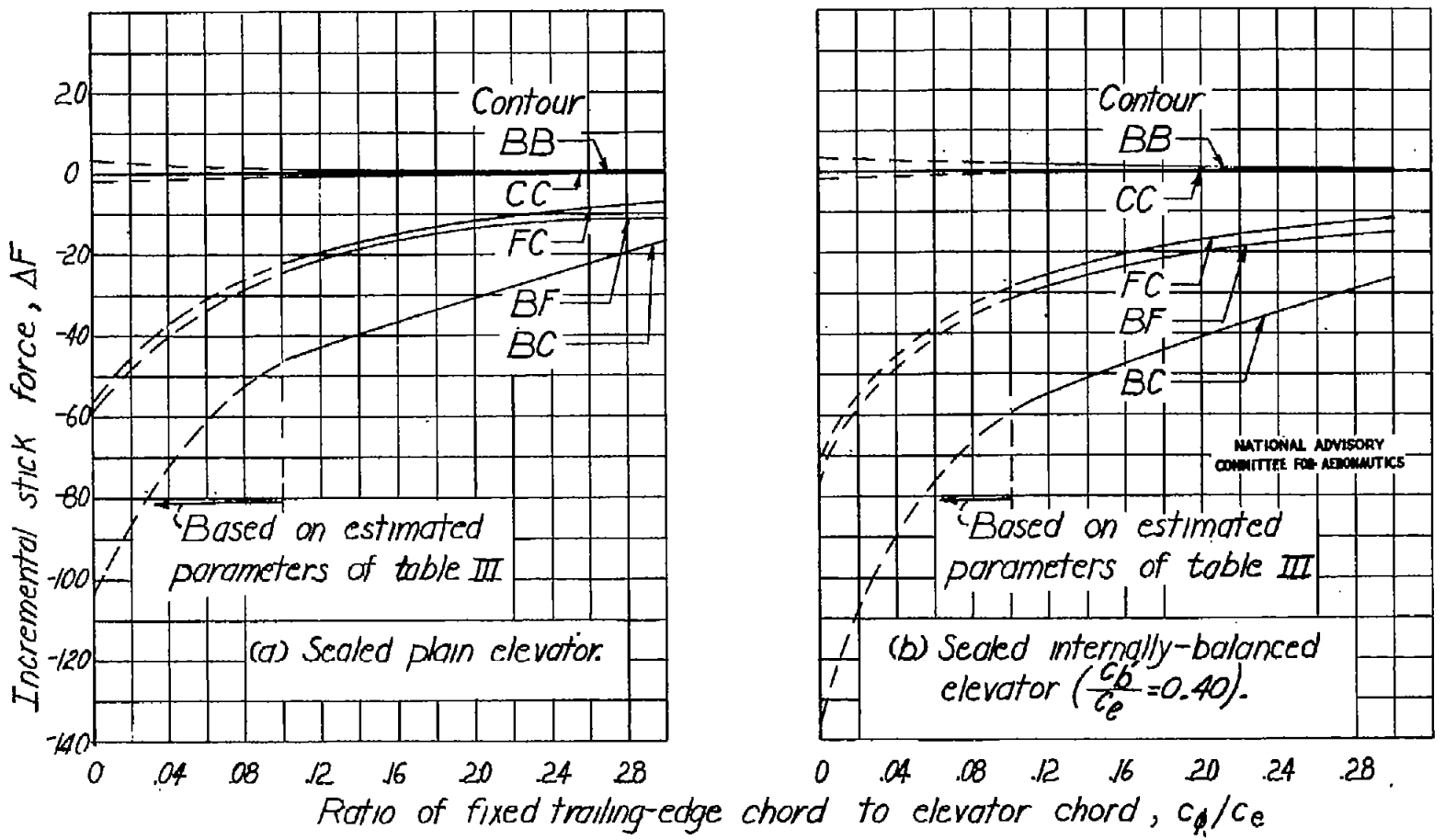

Figure 26.- Effect of the ratio of fixed trailing-edge chord to elevator chord on the incremental stick force, resulting from elevator distortion, required to trim the assumed airplane at a calibrated airspeed of 300 miles per hour. Maximum distortion of each contour equal to 1 percent of elevator chord.